ESTRUCTURACIÓ DE LA RESPOSTA B A LES MALALTIES AUTOIMMUNITÀRIES DE LA TIROIDE

MEMÒRIA DE LA TESI PRESENTADA PER A OBTENIR EL GRAU DE DOCTOR EN CIÈNCIES BIOLÒGIQUES PER LA UNIVERSITAT AUTÒNOMA DE BARCELONA.
BELLATERRA, GENER 2004

Mª del Pilar Armengol i Barnils

10. ANNEX PUBLICACIONS

American Journal of Pathology Vol 159 No 3 September 2001

Thyroid Autoimmune Disease

Demonstration of Thyroid Antigen-Specific B Cells and Recombination-Activating Gene Expression in Chemokine-Containing Active Intrathyroidal Germinal Centers

Maria Pilar Armengol,* Manel Juan,*† Anna Lucas-Martín,† María Teresa Fernández-Figueras,‡ Dolores Jaraquemada,†§ Teresa Gallart,¶ and Ricardo Pujol-Borrell*†

From the Laboratory of Immunobiology for Research and Application to Diagnosis, Centre for Transfusions and Tissue Bank, Endocrinology,† and Pathology‡ Divisions, Hospital Universitari 'Germans Trias i Pujol,' and the Institute for Fundamental Biology,§ Autonomous University of Barcelona, Barcelona, and the Immunology Division,¶ Hospital Clinic i Provincial de Barcelona, Barcelona, Spain*

Autoimmune thyroid disease—Hashimoto thyroiditis and Graves' disease—patients produce high levels of thyroid autoantibodies and contain lymphoid tissue that resembles secondary lymphoid follicles (LFs). We compared the specificity, structure, and function of tonsil and lymph node LFs with those of the intrathyroidal LFs to assess the latter's capability to contribute to autoimmune response. Thyroglobulin and thyroperoxidase binding to LFs indicated that most intrathyroidal LFs were committed to response to thyroid self-antigens and were associated to higher levels of antibodies to thyroglobulin, thyroperoxidase, and thyroid-stimulating hormone receptor. Intrathyroidal LFs were microanatomically very similar to canonical LFs, ie, they had well-developed germinal centers with mantle, light, and dark zones and each of these zones contained B and T lymphocytes, follicular dendritic and interdigitating dendritic cells with typical phenotypes. Careful assessment of proliferation (Ki67) and apoptosis (terminal dUTP nick-end labeling) indicators and of the occurrence of secondary immunoglobulin gene rearrangements (RAG1 and RAG2) confirmed the parallelism. Unexpected high levels of RAG expression suggested that receptor revision occurs in intrathyroidal LFs and may contribute to generate high-affinity thyroid autoantibodies. Well-formed high endothelial venules and a congruent pattern of adhesion molecules and chemokine expression in intrathyroidal LFs were also detected. These data suggest that ectopic intrathyroidal LFs contain all of the elements needed to drive the autoimmune response and also that their microenvironment may favor the expansion and perpetuation of autoimmune response. ***(Am J Pathol 2001, 159:861–873)***

Autoimmune thyroid disease (AITD) is a term that includes the various clinical forms of autoimmune thyroiditis, such as classical Hashimoto's thyroiditis (HT), Graves' disease (GD), and primary myxedema An almost invariable feature of AITD is the production of antibodies to at least one of the main thyroid-specific autoantigens, ie, thyroglobulin (Tg), the main protein of the colloid, thyroperoxidase (TPO), the enzyme that catalyzes iodine organification, and the receptor for thyrotropin (TSH-R) [1] Other thyroid-specific autoantigens, such as the newly described sodium iodine symporter[2] and minor colloid antigens, are still being characterized but they do not seem to be the dominant targets of humoral autoimmune response Thyroid autoantibodies are good clinical markers of disease, and TSH-R antibodies, also known as thyroid-stimulating immunoglobulins, are the direct cause of hyperthyroidism in GD patients and one of the best examples of pathogenic autoantibodies [3] Taking advantage of their high titer, the availability of purified antigens and of surgically removed tissue thyroid autoantibodies were subjected to such an exhaustive scrutiny that they arguably became the best-characterized human autoantibodies A wide variety of techniques have been used, including the generation of human monoclonal antibodies both by hybridoma[4,5] and combinatorial techniques using as source B cells from autoimmune thyroids and the corresponding regional lymph nodes (LNs) [6–8] Epitope restriction typical of human autoantibodies, first suggested for Tg antibodies,[9] has been repeatedly con-

Supported by the "Fondo de Investigaciones Sanitarias (project 98/1123 to M P A and grants 98/1123 and 99/1063)

Presented in part at the second International Autoimmunity Congress Tel Aviv March 8 to 11 1999

Accepted for publication April 13 2001

Address reprint requests to Prof R Pujol Borrell Immunology Unit Hospital Universitari Germans Trias i Pujol Ctra Canyet s/n P O Box 72 08916 Badalona (Barcelona) Spain E mail rpujolb@servet uab es

firmed using human and mouse monoclonal antibodies and recombinant mutated forms of thyroid antigens [10–13] Genetic analysis provided evidence of restricted Ig V gene family usage and extensive somatic hypermutation, as corresponds to high-affinity antibodies produced in the course of antigen-driven responses [12–14] The analysis of the T cell response using a variety of approaches also suggests that AITD is caused by antigen-driven responses [15]

Histologically, HT is characterized by lymphocytic infiltration that may progressively replace thyroid follicles Lymphoid infiltrates are also present in GD glands, but in this condition most of the thyroid remains intact except for the signs of hyperfunction Cases that share features of HT and GD occur are occasionally observed [16] Lymphoid infiltrates often organize themselves as follicle-like structures containing germinal centers (GCs) similar to those in secondary lymphoid follicles (LFs) of LNs Intrathyroidal B lymphocytes can synthesize Tg, TPO, and TSH-R antibodies *in vitro,* and this suggested that they are an important source of thyroid autoantibodies [17–21]

Ectopic or extranodal secondary LFs are found in other autoimmune lesions, such as rheumatoid arthritis synovium,[22–24] myasthenia gravis thymus,[25] and Sjogren's disease salivary glands,[26] but also in chronically infected tissues such as hepatitis C liver[27] and *Helicobacter pylori* gastritis mucosa [28] The formation of extranodal LFs might be a normal development in the course of a maintained immune response but it is not known if it contributes to response effectiveness In autoimmune diseases it has been interpreted as a sign of the intensity of the response but not as a significant step in their pathogenesis The real frequency of lymphoid follicle formation in autoimmune tissue has been difficult to estimate, because these structures are irregularly distributed, scattered all over the affected tissue, and can be easily missed during routine histopathological examination

Lymphoid follicles with GCs are crucial sites in the development of the anamnestic immune responses because they are the sites where cells undergo somatic hypermutation and affinity maturation Newly formed GCs are oligoclonal B cell populations derived from one to three B cell clones [29 30] Somatic hypermutation can generate autoreactive B cells and requires the existence of tolerance mechanisms to keep them under control [31 32] The discovery of RAG and Tdt expression in GCs has suggested that secondary VDJ rearrangement may be another process that contributes to GC function [33–35]

The presence of well-organized B cell structures in AITD glands may be relevant to pathogenesis, not only for the production of autoantibodies but also for the development and maintenance of autoimmune response B cells in intrathyroidal LFs are in a privileged location to capture large amounts of self-antigens and to present them to T lymphocytes It has been suggested that, as they are outside the limits of lymphoid organs, they may bypass normal peripheral tolerance mechanisms more easily [32] The importance of extranodal LF formation for the development of autoimmune disease was established in recent experiments by Ludewig and colleagues[36] using the RIP-GP mouse model, these authors reported a positive correlation between neogenesis of lymphoid tissue and development of autoimmune diabetes The prevention of diabetes in NOD mice incorporating a Igμ null mutation[37] constitutes compelling evidence for the role of B cell in endocrine autoimmune disease

Previous studies by ourselves,[38] and by other authors have described the surprisingly frequent occurrence and complex organization of intrathyroidal LFs This prompted the present study, whose results indicate that intrathyroidal LFs in AITD patients are indeed functional Our data include first evidence that chemokines capable of organizing and self-perpetuating LFs are generated in AITD glands and that secondary rearrangement of immunoglobulin genes may take place in these structures In addition, we have found that intrathyroidal secondary LFs are more prevalent than previously estimated, correlate with autoantibody titer, and seem to result from the expansion of a few seeding B cells that are specific for thyroid autoantigens

Materials and Methods

Patients

Thyroid tissue was obtained from 67 patients, 35 with GD, 8 with HT, 22 with multinodular goiter (MNG), and 2 previously healthy multiorgan cadaveric donors MNG glands were considered nonautoimmune thyroid tissue Clinical diagnosis was based on usual thyroid function tests, including free thyroxine, tri-iodothyronine, and TSH plasma levels TPO and Tg antibodies were measured by enzyme-linked immunosorbent assay (Immunowell, San Diego, CA), normal ranges are 42 to 100 and 67 to 115 IU/ml, respectively Antibodies to TSH-R were measured by radioimmunoassay (Brahms Diagnostica, Berlin, Germany) and all values >1 5 IU/L were considered positive In the statistical analysis, negative samples were assigned the value to the lower limit of detection of the corresponding assay (ie, 24 0, 36 0, and 1 0 IU, respectively) Diagnoses were confirmed by histopathological examination of the glands Tissue samples from one thymus, six palatine tonsils (PTs), and five LNs were used as reference lymphoid tissue

Several blocks from most specimens were treated separately, some were formalin-fixed for standard histopathology tests and other were snap-frozen in isopentane and stored at −70°C Series of sequential cryostat sections (4 μm) obtained from frozen blocks of thyroid, tonsil, thymus, and LN were used for immunofluorescence staining, terminal dUTP nick-end labeling techniques, and also for RNA extraction under RNase-free conditions

Dispersed thyroid cells and intrathyroidal lymphocytes from 42 (26 GD, 3 HT, 13 MNG) glands were prepared by enzymatic digestion as described elsewhere [39] The cells were filtered through a 500-μm mesh and cultured in RPMI 1640, 10% fetal calf serum, and antibiotics Adherent cells, which included thyroid follicular cells, were separated from infiltrating thyroid lymphocytes by adherence to plastic after 18 to 24 hours of culture and separately cryopreserved in fetal calf serum containing 10%

Table 1. List of Lectins and Antibodies Used in the Characterization of Thyroidal GCs

Molecule	Antibody	Source	Host	Isotype
Bcl-2	Bcl-2	Zymed	Mouse	IgG1
CD19	Leu-12	B D	Mouse	IgG1
CD19	A3B1	HCPB	Mouse	IgG2a
CD154	CD154	De-Cheng Shen	Mouse	IgM
CD20	93-1B3	HCPB	Mouse	IgG1
CD20	LE	Dako	Mouse	IgG
CD21L	7D6	P Garrone	Mouse	IgG1
CD23	Leu-10	B-D	Mouse	IgG1
CD3	UCHT1	ATCC	Mouse	IgG1
CD3	Cris-7	HCPB	Mouse	IgG
CD38	RM3A5	HCPB	Mouse	IgM
CD4	RFT4	RFHSM	Mouse	IgG1
CD40	HB14	T F Tedder	Mouse	IgG1
CD5	33-1C6	HCPB	Mouse	IgG2a
CD5	CD5	Caltag	Mouse	IgG1
CD50	101-1D2	HCPB	Mouse	IgG1
CD50	152-2D11	HCPB	Mouse	IgG1
CD54	RM4A3	HCPB	Mouse	IgG
CD71	120-2A3	HCPB	Mouse	IgG1
CD77	38 13	IGR	Rat	IgM
CD79	HM47	HCPB	Mouse	IgG
CD8	RFT8	RFHSM	Mouse	IgG1
CD83	HB15	T F Tedder	Mouse	IgG2
CD95/Fas	DX2	Pharmingen	Mouse	IgG1
CD95L/FasL	NOK-1	Pharmingen	Mouse	
CLA	HECA-452	Pharmingen	Rabbit	IgG
Ki-67	Ki-67	Roche	Mouse	IgG1
FVIII	FVIII	ATCC	Rabbit	
HLA Class I	W6/32	Dakopatts	Mouse	IgG2a
HLA Class II	Edu-1	HCPB	Mouse	IgG2b
hIgD	hIgD	Caltag	Goat	
hIgG	hIgG	Southern-Biotech	Mouse	
hIgM	A1B1	HCPB	Mouse	IgG
hIgs	hIgs	Southern	Goat	
PNA	NO	Sigma	Peanut	NO

BD Becton and Dickinson HCPB, Hospital Clinic i Provincial de Barcelona RFHSM Royal Free Hospital School of Medicine IGR Institut Gustave Roussy

dimethyl sulfoxide The lymphocyte-to-thyroid follicular cell ratio was assessed by fluorescence-activated cell sorting as described elsewhere [39]

Identification of Germinal Centers, Immunofluorescence Staining, and Image Analysis

Thyroid blocks, with an average weight of 5 g, were systematically screened for LFs by examining 1 out of 10 sequential cryostat sections stained by hematoxylin and eosin (H&E) and confirmed by either immunofluorescence staining with peanut agglutinin and anti-IgD (cryostat sections)[40] or with anti-CD20 (formalin-fixed sections) Ten to 80 consecutive 4-μm sections were stained for phenotypic markers, adhesion molecules, and related functional markers by simple or double-indirect immunofluorescence or by immunohistochemistry technique following published protocols[41] and using the antibodies listed in Table 1 Epithelial cells were identified with high titer (1 10^5) anti-TPO patient's serum Affinity-purified fluorochrome-labeled conjugated antisera (specific for some IgG subclasses) were used as secondary antibodies (all from Southern Biotechnology, Birmingham, AL) In all cases, the controls included both using nonimmune sera or unrelated mAb as primary antibodies and testing the effect of omitting each of the layers Biotin-labeled TPO and Tg (a kind gift from Pharmacia-Upjohn, Freiburg, Germany) and fluorescein isothiocyanate-streptavidin were used to detect B and plasma cells bearing Ig that were specific for these antigens The controls included blocking staining with unlabeled antigens

The slides were examined blindly by two independent observers (MPA and RPB or MJO), using either UV or transmitted light microscopy (Axioplan II, Zeiss, Wetzlar, Germany) To better compare the distribution of different markers in some double-immunofluorescence experiments, photomicrographs of the red and green fluorescence images were digitized and then superimposed using commercial software (Photoshop, Adobe, San Jose, CA) Images from some preparations were acquired and deconvolved using a digital confocal microscopy system (Openlab, Improvision, Coventry, UK) to improve resolution but natural colors were maintained The figure legend indicates whether the images have been processed To compare better the LFs from thyroid autoimmune glands, LNs and tonsils, we measured the GC and mantle zone (MZ) areas, the perimeter, and the maximal and minimal diameters using the Openlab morphometry module

TdT-Mediated dUTP Nick-End Labeling Assay

Apoptosis was detected by using a commercial kit (*In situ* cell death detection, Boehringer Mannheim, Mannheim, Germany) following the manufacturer's instructions Two substrates were used and the protocol was adjusted accordingly, 1) sections from formalin-fixed paraffin-embedded blocks (4 μm) were dewaxed, rehydrated, and digested with proteinase K (20 μg/ml), and 2) cryostat sections (4 μm) were fixed in 4% paraformaldehyde and permeabilized with 0 1% Triton X-100/0 1% sodium citrate solution dNTP-fluorescein isothiocyanate was detected with an anti-fluorescein alkaline phosphatase-conjugated antiserum and Fast red The sections were counterstained with Mayer's hematoxylin for 30 seconds Apoptotic nuclei were counted using the Openlab software and expressed as number of positive nuclei per mm^2

Microdissection, RNA Extraction, and Reverse Transcriptase-Polymerase Chain Reaction (RT-PCR) Amplification

To study the RNA from the LFs, these structures were identified by H&E staining and microdissected from 4 to 10 consecutive thyroidal sections under a stereomicroscope (SV8, Zeiss) RNA was extracted from sections devoid of LFs and from control normal lymphoid organs To study chemokine expression, RNA was extracted from frozen tissue blocks Genomic DNA was removed by digestion with DNase-I and the RNA was reprecipitated with 0 4 μmol/L of nuclease-free glycogen (Boehringer-Mannheim) as a carrier, then, it was quantified in a spectrophotometer at $OD_{260\ nm}$ cDNA was prepared in a final volume of 10 μl by mixing 200 ng to 1 μg of total RNA, 20 pmol Oligo-(dT_{15}) (Pharmacia-Biotech), 40 U/μl RNase inhibitor (Clontech), 10 mmol/L dNTP mix (Pharmacia-Biotech), 0 1 mol/L dithiothreitol (DTT), 1× SuperScript buffer and 200 U/μl of SuperScript-II enzyme For RAG2, the antisense primer used for the retrotranscription and for PCR amplification was the same The reaction was performed at 42°C for 45 minutes and the product was diluted 5 to 10 times in TE (10mM TRIS/1mM EDTA, (TE) pH 8) for subsequent experiments For PCR reactions 1 to 3 μl of cDNA was added to the mixture containing 0 2 mmol/L dNTP, 0 3 μmol/L each primer, 1× PCR buffer and 300 mU of DynaZyme II (Finnzymes, Oy, Finland) to a final volume of 20 μl in hot start The following programs and primers were used 1) GAPDH, 30 cycles at 94°C for 30 seconds, denaturation, 65°C for 45 seconds, annealing/elongation (sense primer 5′-TCTTCTTTTGC GTCGCCAG-3′, antisense primer 5′-AGCCCCAGCCTTCTCCA-3′), amplicon 371 bp 2) RAG1 35 cycles at 94°C for 30 seconds, denaturation, 56°C for 30 seconds, annealing at 72°C for 40 seconds, elongation (sense primer 5′-ACTTTCCCTTCATCCTGCTTA-3′, antisense primer 5′-TTTTTCTCCTCCTCTTGCTTC-3′), amplicon 653 bp 3) RAG2, 30 cycles of denaturation at 94°C for 30 seconds, annealing at 63°C for 30 seconds, extension at 72°C for 40 seconds (sense primer 5′-GCCACAGTCATAGTGGGCAGTCA G-3′, antisense primer 5′-CAAAGGGAGTGGAATCCCCTGG-3′), amplimer 534 bp 4) SDF-1, 30 cycles of denaturation at 94°C for 30 seconds, annealing at 60°C for 20 seconds, and extension at 72°C for 30 seconds (sense primer 5′-GTCGTGGTCGTGCTGGTC-3′, antisense primer 5′-CGGGCTACAATCTGCAGG-3′), amplicon 155 bp 5) SLC, 35 cycles at 94°C for 30 seconds, denaturation, 65°C for 45 seconds annealing/elongation (sense primer 5′-AAGGCAGTGATGGAGGGG-3′, antisense primer 5′-CTGGGCTGGT TTCTGTGG-3′), amplicon 238 bp 6) BLC, 35 cycles at 94°C for 30 seconds, denaturation, 51°C for 20 seconds, annealing at 72°C for 30 seconds, elongation (sense primer 5′-CGACATCTCTGCTTCTC-3′, antisense primer 5′-ACTTCCATCATTCTTTG-3′), amplicon 255 bp All amplifications were followed by a final extension at 72°C for 7 minutes The PCR products were analyzed by 1 to 3 5% agarose gel electrophoresis and transferred to nylon membranes (Hybond+, Amersham) The membranes were hybridized with specific labeled probes [γ-^{32}P]ATP 10μCi/μl) at high stringency conditions (RAG1 5′-CCCTTACTGTTGAGACTGC-3′, RAG2 5′-GGACAAAA AGGCTGGCCCAA-3′, SDF-1 5′-TGCCTCAGCGACGGG-3, SLC 5′-CTTGGTT CCTGCTTCCG-3′, BLC 5′-ACAACCATTCCCACGG-3′) In the case of RAG1, both primers annealed to the same exon (exon 2) so a sample of unretrotranscribed RNA was introduced as an additional control To estimate the amount of chemokine message in tissue samples, hybridized membranes were exposed and the autoradiographies were either counted on a Phosphorimager (BioRad, Richmond, CA) using Quantity One software or assessed by densitometry (TDI Systems) The results were normalized according to the amount of GAPDH message as estimated by densitometry of gels stained with ethidium bromide Preliminary experiments were performed to establish the conditions under which the reactions were within the exponential phase of amplification To better compare the levels of the different chemokines and refer them to a physiological substrate, the values obtained from thyroid samples were divided by the average value from PT for each chemokine Therefore, the results are given as percentages of reference PT values

Statistical Analysis

Data distribution was first analyzed using the Sigma Stat software (Microsoft Corp , Seattle, WA) Parametric (Student's *t*-test) and nonparametric (Mann-Whitney) tests were applied to normal and nonnormally distributed data, as indicated

Results

Most AITD Glands Contain Typical Secondary Lymphoid Follicles that Are Large and Tonsil-Like in HT and Smaller and Lymph Node-Like in GD

Typical secondary LFs, similar to those found in lymphoid organs were easily detected by screening H&E sections

Table 2. Classification of Thyroid Glands According the AITD, Autoantibody Titers, Percent of Leukocyte Infiltration and Presence of Germinal Centers

Sample	AITD	αTg UI/ml	αTPO UI/ml	αTSHR UI/l	% LI	S (N of GC)
228	GD	-ve	-ve	80 0	ND	1 (11)/2 (1)
255	GD	-ve	25	20	ND	1 (1)
257	GD	598 0	1155 0	67 0	70 2	1 (3)
258	GD	-ve	-ve	118 0	ND	1 (1)
278	GD	-ve	-ve	16 0	ND	1 (1)
373	GD	172 1	39 2	178 0	27 7	1 (1)
378	GD	177 3	152 3	1 0	30 0	1 (1)
381	GD	162 8	48 1	ND	19 5	NO
389	GD	66 8	143 6	37 5	9 6	NO
390	GD	28 3	-ve	8 4	7 03	NO
391	GD	ND	25	ND	4 9	NO
393	GD	35	42 0	62 0	43 4	1 (1)
394	GD	-ve	43 5	38 0	4 8	NO
403	GD	36	550 0	-ve	38 8	2 (3)
412	GD	239	124 3	8 8	20 0	1 (4)
413	GD	37 2	39 4	20 6	5 2	NO
416	GD	56 4	40 5	-ve	9 2	NO
417	GD	-ve	25	75 0	9 5	NO
423	GD	70	53	15 5	10 2	NO
424	GD	-ve	-ve	4 1	54 5	NO
425	GD	-ve	28	4 0	11 4	NO
426	GD	1265	1001	85 9	45 4	1 (2)?
427	GD	190	1001	14 9	ND	1 (1)
429	GD	-ve	7000	-ve	50	3 (2)
430	GD	-ve	46	10 1	10 6	1 (1)
290	HT	584 0	766 0	-ve	ND	2 (1)
384	HT	ND	ND	ND	66 6	1 (5)
385	HT	774 0	105000	-ve	76 6	1 (1)
BL	HT	ND	ND	ND	ND	1 (10)
JC	HT	ND	ND	ND	ND	1 (5)
RP	HT	ND	ND	ND	ND	1 (10)
AP1	HT	ND	ND	ND	ND	1 (4)
AP2	HT	ND	ND	ND	ND	1 (11)
359	MNG	-ve	-ve	-ve	5 2	NO
360	MNG	-ve	-ve	2 5	1 3	NO
361	MNG	-ve	-ve	7	0 3	NO
362	MNG	-ve	-ve	1 6	6 1	NO
364*	MNG	-ve	-ve	1 2	12 0	1 (1)
376	MNG	-ve	37 9	1 4	3 5	NO
379	MNG	-ve	-ve	1 2	6 8	NO
395	MNG	-ve	-ve	-ve	7 2	NO
396	MNG	-ve	36	-ve	3 9	NO
399	MNG	-ve	45 9	1 2	21 7	NO
409	MNG	27 5	41	-ve	20 6	NO
419	MNG	36	23	-ve	11 7	NO
420	MNG	-ve	-ve	-ve	7 5	NO

GD Graves disease HT Hashimoto thyroiditis MNG multinodular goitre % LI percentage of lymphocytic infiltration S (N of GC) sections (number of GCs)

Eight of 8 (100%) glands from HT, 14 of 26 (53 8%) from GD, and 1 of 22 (4 5%) from MNG patients contained LFs (Table 2)

Intrathyroidal secondary LFs possessed a MZ and well-formed GCs with obvious signs of activity (eg, lymphoblasts in mitosis) The GCs appeared in areas of heavy infiltration, but relatively isolated GCs were also found, and often they were so close to the thyroid follicles that the mantle lymphocytes were adjacent to the thyroid epithelium Nests of epithelial cells often remained in the middle of dense infiltrates, apparently unaffected by the surrounding lymphocytes The cells forming the intrathyroidal GCs were polarized in a dark zone containing lymphoblasts with big nuclei and two or three nucleoli, and a light zone surrounded by small lymphocytes with the features of centrocytes Large dendritic cells with elongated nuclei were present in the GC and the MZ, whereas plasma cells were scattered all over the infiltrate (Figure 1a) This cellular distribution was confirmed by staining for a series of phenotypic markers Among them, anti-CD20 (Figure 1b) and peanut agglutinin-fluorescein isothiocyanate (Figure 1c) specifically labeled the GCs Peanut agglutinin stained both the GCs and the vascular endothelium, a feature that was useful to trace a given GC in consecutive sections The MZ consisted of typical CD19low IgD+ IgM+ CD38− CD23−/low+ follicular B lymphocytes (data not shown), but some areas were rich in CD3+ cells, predominantly of the CD5+ CD3+ $CD4^+$ phenotype but also containing CD3+ CD8+ cells, these areas corresponded to the T-cell rich MZ areas observed in lymphoid node LFs (Figure 1, d, e, and f) Staining for CD83 (Figure 1g) revealed a rich network of DCs that

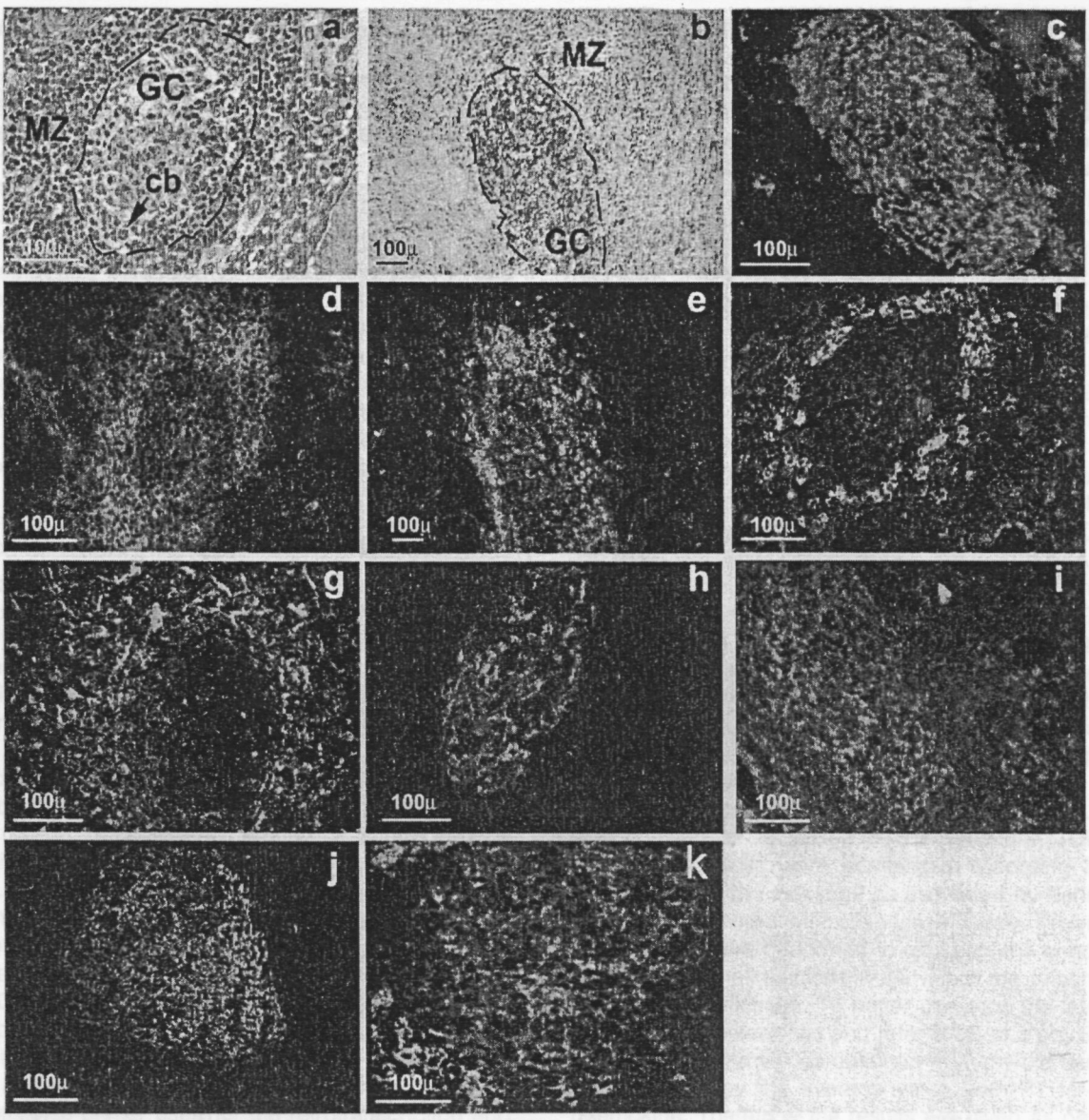

Figure 1. Morphology of intrathyroidal secondary LFs in AITD. **a:** A section from a formalin-fixed paraffin-embedded block from a HT gland. **b** to **h:** Sections from frozen blocks from GD glands. **g** was deconvolved to improve image definition (see text for details), the other images are standard micrographs. **a:** H&E staining showing a typical secondary follicle with a GC and a well-formed MZ (cb, centroblasts undergoing mitosis). **b:** CD20 on B cells of the GC (brown) using the immunoperoxidase technique and counterstained with hematoxylin (GD, case TB228). **c:** Direct immunofluorescence with peanut agglutinin-fluorescein isothiocyanate, showing positive staining of centroblasts and follicular dendritic cells (GD, case TB378). **d:** Staining for CD3+ reveals abundant T cells in the MZ with scattered cells inside the GC (GD, case TB228). **e:** Demonstration of abundant $CD4^+$ T among the T cells in the MZ (GD, case TB228). **f:** Staining for CD8 shows moderately abundant CD8+ T lymphocytes in the MZ (GD, case TB378). **g:** Staining for CD 83 highlights the network of mature dendritic cells in the MZ (GD, case TB278). **h:** Staining for the long form of CD21 reveals the network of follicular dendritic cells in the CG and their polarization toward the light zone (GD, case TB373). **i:** CD38, as marker of centrocytes. **j:** CD23 staining revealing the area occupied by the GC. **k:** CD77 staining as an additional GC marker .

included extensive areas of the MZ and of the surrounding infiltrate, but normally did not reach the inner GC area. Immunofluorescence staining confirmed the presence within the GC of the two characteristic B cell populations: IgM−/low IgD− CD23− CD77+ CD38+ centroblasts and CD77+ CD38+ CD23+ centrocytes. A framework of follicular dendritic cells, polarized toward the light zone, was identified by mAb 7D6 against the long form of CD21(CD21L) (Figure 1h).

LFs from different glands were found to differ in size and complexity, and a correlation with diagnosis was quickly discovered. LFs in HT glands were large and similar to LFs in tonsils, whereas LFs in GD glands were smaller and similar to LN LFs. The measurement of 122 LFs from a random selection of samples (26 in tonsil, 39 in LN, 20 in GD, 37 in HT samples) confirmed this fact (Figure 2). GC and LF areas in GD and HT glands were significantly different ($P = 0.0020$ and $P = 0.0174$, respectively, *t*-test). As expected, the presence of LFs was associated by the presence of extensive lymphoid infiltration ($P < 0.000005$, Mann-Whitney). LFs were detected in heavily infiltrated glands (defined as containing >25% of lymphocytes over total amount of dispersed cells, as assessed by flow cytometry of 24-hour thyroid

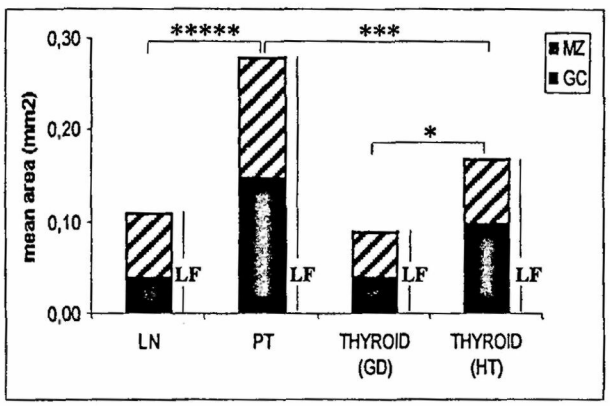

	GC	MZ	LF
LN	0.043±0.02	0.017±0.02	0.113±0.05
PT	0.148±0.05	0.128±0.08	0.275±0.08
GD	0.042±0.05	0.054±0.04	0.096±0.09
HT	0.102±0.09	0.065±0.06	0.166±0.12

Figure 2. Morphometric analysis of LFs from HT and GD compared with LFs from LNs and PTs. **Solid bar**, area occupied by the GC; **hatched bar**, area occupied by the MZ. Number of LFs studied: LNs, 39; PTs, 26; GDs, 20; and HTs, 37. The **asterisks** indicate significant differences between total LF areas: ****, $P < 0.001$; ***, $P < 0.00.5$; *, $P < 0.05$. The table below gives numerical values ± SD.

primary cultures (data not shown), but this relationship was not symmetrical; some glands with extensive infiltration lacked LFs.

AITD Intrathyroidal Lymphoid Follicles Are Committed to TPO and Tg Antibody Production

Both in the whole study group and in the AITD group, the presence of intrathyroidal LFs was associated to significantly higher levels of TPO ($P = 0.00860$, Mann-Whitney test) but not of Tg autoantibodies, although a tendency toward association was observed ($P = 0.053$). In the GD group, intrathyroidal LFs were associated to higher levels of TSH-R antibodies ($P = 0.0146$, Mann-Whitney test). The specificity of the B cells in intrathyroidal LFs was demonstrated by the binding of Tg and TPO to LFs in a HT gland (16 of 28 LFs) and in four GD glands (17 of 27; Figure 3b). Two types of cells bound thyroid antigens: numerous small cells with a distribution similar to that of GC B cells and strongly positive cells with a strong cytoplasmic staining scattered all over the LFs and the diffuse lymphoid infiltrates. Double immunofluorescence revealed that most cells that bound to TPO or Tg were IgG+. The distribution of Tg+ or TPO+ cells was markedly uneven among the LFs, which tended to either be totally negative or contain numerous positive cells. This suggested that, as in canonical LFs, intrathyroidal CGs consist of an oligoclonal B cell population. Blocking experiments with unlabeled TPO and Tg gave negative results, thus confirming the specificity of the reaction.

AITD Lymphoid Follicles Express the Molecules Required for Secondary Lymphoid Follicle-Specific Processes, Including Recombinase-Associated Gene Products RAG1 and RAG2

Proliferation in the LFs is linked to somatic hypermutation and Ig repertoire diversification. AITD GCs contained many cells positive for the proliferation marker Ki67, which were oriented toward the dark zone; this was also the case in control tonsil and LN tissue samples (Figure 4a). Two-color immunofluorescence with anti-IgM antibodies confirmed that most Ki67-positive cells were lymphoblasts with slight or no IgM staining. Cell proliferation is high in AITD GCs, especially in HT glands; the level of proliferation is similar to that detected in tonsil GCs and well above that of LNs (Figure 4b). Collaboration between B and T lymphocytes through CD40-CD40L interaction is central to GC functions.[42] As in lymphoid LFs,[43] intrathyroidal LFs contained in their GCs a small polarized population of CD40+ B cells and some scattered B lymphocytes bearing the IgD+CD38−CD40L+ phenotype in the T-cell-rich area. CD40 was expressed by a population of large-sized dendritic cells located outside the LFs, in the areas of diffuse lymphocytic infiltration where T lymphocytes predominate. These cells probably correspond to the dendritic cells stained by CD83 in other sections and are equivalent to the dendritic interdigitating cells described in the paracortical area of LNs (data not shown).

Apoptosis, which is an intrinsic feature of LN GCs, was detected by the terminal dUTP nick-end labeling technique in intrathyroidal LFs, especially in those from HT glands (Figure 4c). Positive nuclei were located mainly in the light zone, but some labeled nuclei were detected in the rest of the GC areas as well as outside them, but not in the thyroid follicular epithelium, as reported.[44] The number of apoptotic cells per square mm in LFs from HT was as high as in the tonsils (370.2 ± 186 *versus* 325 ± 99.4; P = not significant) and significantly higher than in GD glands (126.4 ± 57.6) (HT *versus* GD; $P < 10^{-4}$, *t*-test). B-lymphocyte apoptosis in lymphoid organ LFs is triggered by CD95-CD95L (Fas/FasL) interaction and is modulated by the expression of Bcl-2 and other anti-apoptotic factors. As expected, centroblasts were Fas+ Bcl2− (Figure 4, d and f) whereas most centrocytes were Fas− Bcl-2+. The IgD+ naïve B cells in the MZ were also bcl-2-positive. In general, the distribution of these two molecules was similar to that observed in tonsils and LNs, but in intrathyroidal LFs the level of Bcl-2 seemed to be higher than in lymphoid organ LFs.

It has been reported that the RAG1 and RAG2 recombinase genes are expressed in secondary lymphoid organs during active immune response (see Discussion). We assessed the expression of RAG1 and RAG2 in AITD glands by RT-PCR and Southern blotting using thymus, tonsil, and LN as positive controls. RNA was extracted from 4 to 10 consecutive cryostat sections and, when feasible, intrathyroidal GCs were microdissected. All sec-

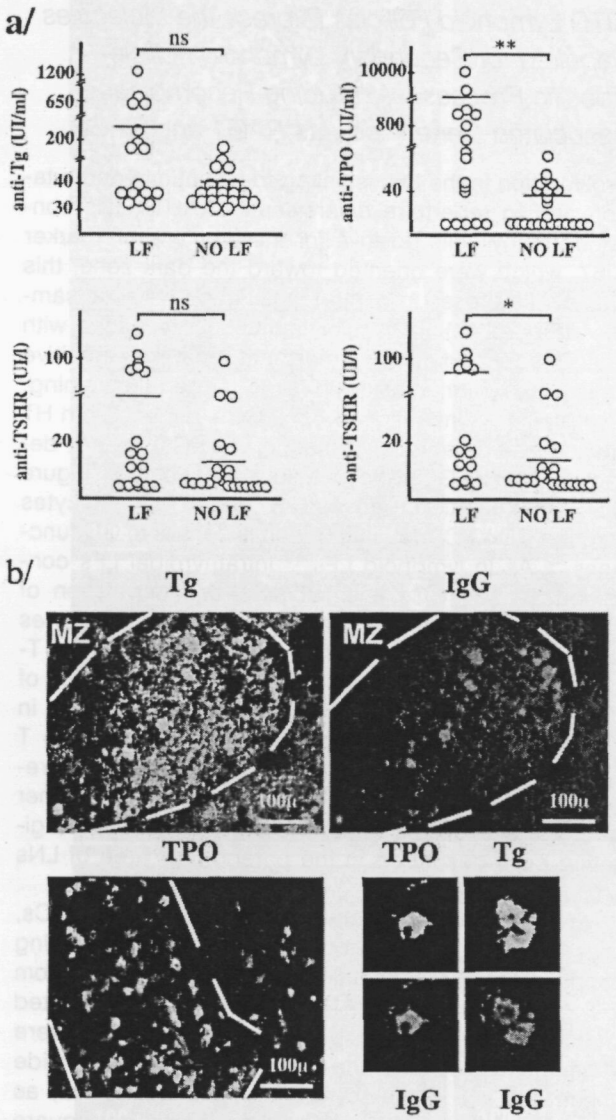

Figure 3. a: Relationship between thyroid antibody titer and the presence of intrathyroidal LFs. TSHR, thyrotropin receptor; LF, group of thyroid glands containing LFs; NO LF, group of thyroid glands without LFs. The plotted data, except for those at **bottom right**, correspond to all of the patients in Table 2. At the **bottom right**, only the data from GD patients were plotted (*, $P < 0.05$; **, $P < 0.01$; ns, not significant P value, Mann-Whitney test). **b:** Demonstration of the specificity of B and plasma cells in the intrathyroidal LFs. Double immunofluorescence using biotinylated Tg (green, **top left**) and anti-IgG (red, **top right**), demonstrating binding of Tg to the same cells that are stained for IgG. Positive lymphocytes only appear in the LFs, whereas plasma cells are present both in the LFs and in the diffuse infiltrate. **Bottom left:** Binding of biotinylated TPO to abundant cells in the LFs and also to some cells in the diffuse infiltrate. Note the presence of membrane and cytoplasmic staining that correspond to lymphocytes and plasma cells, respectively. **Bottom right:** Examples of plasma cells stained for TPO and Tg in double immunofluorescence with IgG (GD, case 378).

tions containing GCs were positive for RAG1 and RAG2 (HT, $n = 3$; GD, $n = 4$) irrespective of diagnosis, whereas sections that did not contain GCs were negative (HT, $n = 1$) (Figure 5). Based on partially normalized densitometric data, the levels of RAG1 and RAG2 mRNA levels in most glands containing LFs were several times higher than in tonsil and LN samples, and in some cases higher than in samples from the thymus. Tissue samples obtained from the same glands but without LFs showed lower RAG1

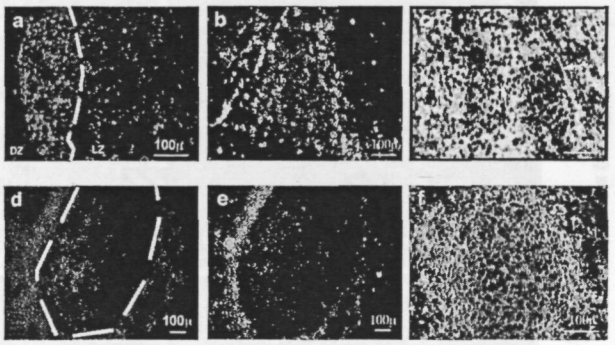

Figure 4. Proliferation and apoptosis in thyroid LFs. **a:** Immunofluorescence staining for Ki67 in an intrathyroidal LF, showing abundant proliferating cells polarized toward the dark zone (GD, case TB228). **b:** Double-immunofluorescence staining for IgD (green) and Ki67 (red), demonstrating that most proliferating cells are in the light zone of the GC and are either negative or slightly positive for IgD, as in the case of centroblasts. **c:** Demonstration of the existence of apoptotic cells by the terminal dUTP nick-end labeling technique and hematoxylin counterstain. Most positive cells were found in the GC area; no positive cells were seen in the epithelium of the thyroid follicles (data not shown). **d** and **e:** Double immunofluorescence for bcl-2 and IgD. The level of expression of apoptosis inhibitor bcl-2 is high in the MZ but is also expressed in the GC cells. The staining for IgD shows the distribution of mature B cells in the MZ. **f:** Double exposure of double-immunofluorescence staining for IgD (green) and CD95/Fas (red). Notice that Fas is mainly expressed in the CG, whereas IgD is expressed in the MZ, as is the case in normal LNs.

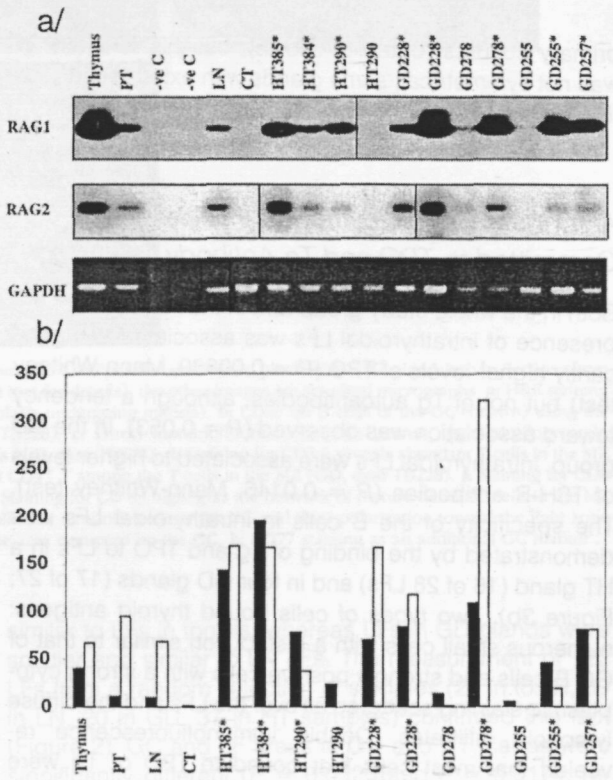

Figure 5. RAG1 and RAG2 mRNA expression measured by RT-PCR Southern blot in HT and GD glands. **a:** Southern blot of RT-PCR products amplified with RAG1 and RAG2 primers and hybridized with the corresponding oligoprobes; **bottom**, RT-PCR for control GAPDH; only partial normalization was achieved because of the small amount of available sample. **Asterisks** indicate samples that contained visible GCs. TMB, thymus; CT, esophagus. **b:** Graph representing the ratio of densitometry values: RAG1, GAPDH (**solid bars**); RAG2, GAPHDH (**open bars**), using an inverted image of the GAPDH gel image.

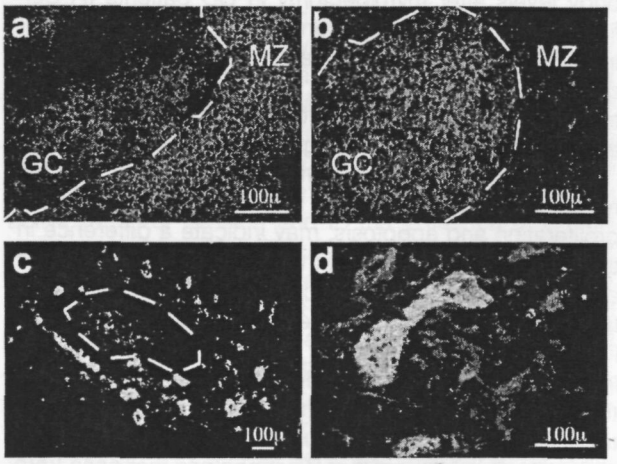

Figure 6. Distribution of adhesion molecules in the thyroidal LFs. **a:** ICAM-1 membrane staining is mainly present in the MZ cells. **b:** ICAM3 expression is higher in cells inside the GC and has a reticular pattern similar to that observed for the follicular dendritic cells. **c:** CD62L-positive HEVs are distributed around the LF. **d:** Picture resulting from superimposing digitized images for CLA (green) and Factor VIII (red) staining in the same section. Note that the large vessels are positive for both markers, thus indicating the location of the HEV. Cryostat sections from GD, case TB278.

and RAG2 levels. There were no clear differences between HT and GD glands.

AITD Lymphoid Follicles Express the Adhesion Molecule and Chemokines Required for Self-Perpetuation as Homing Area

These two categories of molecules determine the development, organization, and self-perpetuation of LFs in the lymphoid organs. The distribution of ICAM-3 (CD50) and ICAM-1 (CD54) was similar to that observed in LN LFs,[45] ie, ICAM-3 was expressed mainly in the MZ and the surrounding area and in a few cells of the GC (both centroblasts and centrocytes), whereas ICAM1 was expressed by GC cells and especially in the follicular dendritic cell-rich area (Figure 6). The distribution of CLA (cutaneous lymphocyte-associated antigen), a carbohydrate domain that is the ligand for L-selectin (CD62L) and a marker for high endothelial venules (HEVs),[46] was studied in parallel with that of factor VIII, an endothelial marker.[38] In the rich capillary network that surrounds the intrathyroidal LFs revealed by FVIII staining, ~20% of the endothelial cells (Figure 6, c and d) were positive for CLA (Figure 6e). Besides, occasional CD3+ CLA+ were detected in the areas of lymphoid infiltration. The endothelium of MNG and GD thyroids lacking LFs was either completely negative or only showed a very low expression of CLA.

The expression of chemokines known to be important for the formation and maintenance of GCs [ie, stromal cell-derived factor 1 (SDF1 or CXCL12), secondary lymphoid tissue chemokine (SLC or CCL21), and B lymphocyte chemoattractant/B-cell-attracting chemokine 1 (BLC/BCA-1 or CXCL13)], was assessed by semiquantitative RT-PCR. A small selection of glands containing LFs was selected, RNA samples were prepared from total

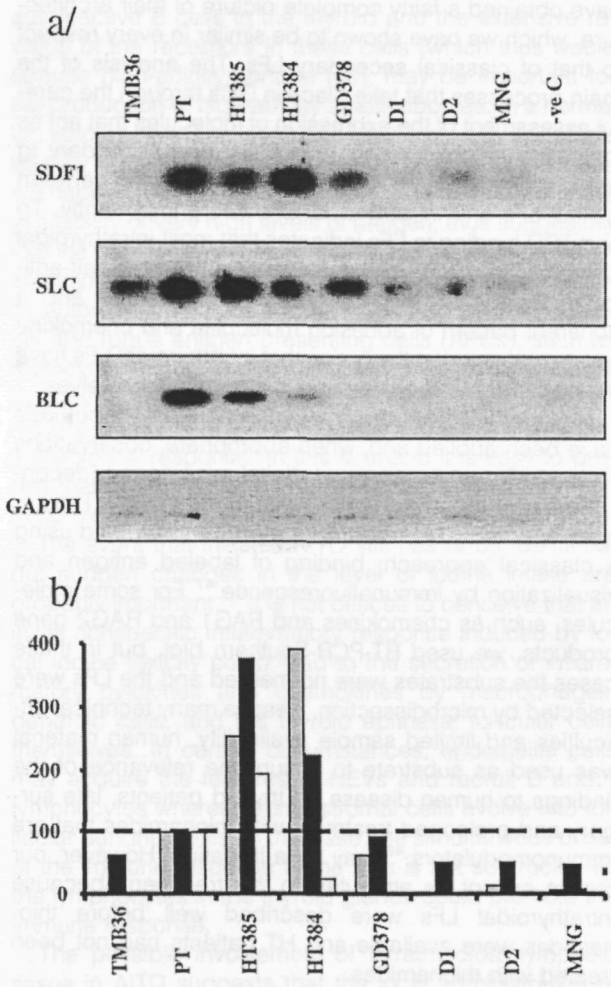

Figure 7. Chemokine expression as assessed by RT-PCR-Southern blot and phosphorimager counting. **a:** RT-PCR-Southern blots. **b:** Ratio for normalized chemokine value in each gland: normalized tonsil value, ×100; the **broken line** at 100% represents the tonsil reference value. **Gray bars**, SDF1 (CXCL12); **solid bars**, SLC (CCL21); **open bars**, BLC (CXCL13). TMB, thymus; D1 and D2, normal donors.

tissue and retrotranscribed as described above. Figure 7a shows the results from one representative amplification experiment. mRNA from the three chemokines was detected in the positive control and their level of expression was clearly high in the two HT samples. Because the cDNA samples had been normalized by GADPH expression, the observed fourfold increase of SLC and SDF1 levels over PT levels indicates a remarkably active synthesis of chemokine message in the HT glands. BLC message was also higher, but only when compared to normal or MNG thyroid tissue. In the GD gland studied, chemokine expression was not different from that in normal or MNG tissue (Figure 7b).

Discussion

Secondary LFs have been studied so intensively in the last decade that it is not feasible to reproduce here even a small fraction of these studies on intrathyroidal LFs. However, by using a series of phenotypic markers we

have obtained a fairly complete picture of their architecture, which we have shown to be similar in every respect to that of classical secondary LFs The analysis of the main processes that take place in GCs through the careful assessment of the expression of molecules that act as indicators of proliferation, apoptosis, and secondary Ig gene rearrangement confirmed the similarity between typical LFs and intrathyroidal LFs More importantly, Tg and TPO binding to LFs indicates that most intrathyroidal LFs are committed to the response to thyroid self-antigens Finally, the finding of well-formed HEVs and a coherent pattern of adhesion molecules and chemokine expression support the notion that intrathyroidal LFs have the capability to organize and perpetuate themselves

Histopathological and immunohistochemistry methods have been applied and, when appropriate, observations were confirmed by confocal digital microscopy (deconvolution-based) and computerized morphometry The antigen specificity of B and plasma cells was studied using a classical approach binding of labeled antigen and visualization by immunofluorescence [47] For some molecules, such as chemokines and RAG1 and RAG2 gene products, we used RT-PCR-Southern blot, but in these cases the substrates were normalized and the LFs were selected by microdissection Despite many technical difficulties and limited sample availability, human material was used as substrate to ensure the relevance of the findings to human disease In thyroid patients, late surgery and prolonged treatment with thionamides that are immunomodulators,[48] may be a limitation However, our results cannot be attributed to this treatment, because intrathyroidal LFs were described well before thionamides were available and HT patients had not been treated with thionamides

The presence of intrathyroidal LFs in AITD was considered to be a very characteristic feature of HT but not of GD By their nature, LFs are scattered over the thyroid gland and can be easily missed, especially in GD, where infiltration is much less intense By using a screening protocol that takes into account the average size of LFs and checking 1 in 10 sections, the possibility of missing LFs was reduced to the minimum However, because we did not screen >5 g of each gland, our data could still be an underestimate It is plausible that, if the entire glands had been screened, the frequency of LFs in GD would have been higher, thus implying that LFs are a regular feature The association between high titer of antibodies against TPO and TSH-R and the presence of intrathyroidal LFs in AITD glands suggests that these structures play a role in antibody production One possibility is that the formation of intrathyroidal LFs determines transition from self-limited responses to thyroid antigens to AITD, as suggested by the experimental model of Ludewig and colleagues [36] Our results showed binding of Tg and TPO to B and plasma cells, and their distribution among LFs suggests that most intrathyroidal LFs are actually committed to thyroid antigen immune response The elucidation of the relative contribution of intrathyroidal LFs to the circulating levels of thyroid autoantibodies requires experiments that are difficult to justify in human patients, but the clinical observation of a quick reduction in autoantibody levels after thyroidectomy in GD patients (A Belfiore, personal communication),[49] suggests that this contribution is important If the autoimmune response was driven from the regional LNs, the persistence of antigen trapped in their follicular dendritic cell[50] would maintain the response for a much longer period of time

The similarity of HT and GD LFs to PTs and LN LFs, respectively, similarities that also apply to the levels of proliferation and apoptosis, may indicate a difference in the pathogenesis of each of these two forms of AITD PTs and intrathyroidal HT LFs show a high degree of activation It has been reported that PT LFs are activated by lipopolysaccharide and other bacterial products present in the pharynx [51] Current evidence and our data suggest that intrathyroidal LFs are stimulated by high concentrations of thyroid proteins, thus explaining their state of activation It is relevant that B lymphomas that arise from HT glands have features similar to those of the MALT lymphomas,[52] which are caused by monoclonal expansion of B cells chronically stimulated by antigens of the gastrointestinal tract Similarly, B lymphomas in HT patients, which are histopathologically similar to the MALT lymphomas, could result from chronic stimulation of GC lymphocytes by thyroid autoantigens [53] The intrathyroidal LFs from GD patients are less active, and this may be because of a lower concentration of TSH-R, the most important self-antigen in this entity Besides, as TSH-R is also expressed outside the thyroid,[3] the response to it may be less dependent on intrathyroidal stimulation In fact, it has been proposed that GD is a systemic disease [54]

The complete parallelism between intrathyroidal LFs and secondary LFs in peripheral lymphoid organs suggests similar functional capabilities, probably including those not specifically studied in this work, such as Ig class switch RAG1 and RAG2 expression, the visualization of HEV and the detection of the main chemokines that determine the organization of LFs have not been reported before and need to be discussed

The RAG1 and RAG2 recombination activation genes play a central role in the rearrangement of V(D)J gene segments during lymphocyte development in the primary lymphoid organs [55] The finding of RAG1 and RAG2 expression in splenic B cells stimulated *in vitro* with LPS+IL-4 and in GC B cells of immunized mice suggested that at least some peripheral B cells can be induced to re-express or up-regulate these genes [33 34 56–58] This RAG re-expression was initially interpreted as evidence for the occurrence of peripheral receptor editing (receptor revision) aimed at rescuing autoreactive B cells generated by somatic hypermutation The demonstration that Ig cross-linking inhibited RAG expression in human tonsil B cells led to the suggestion that receptor revision was rather aimed at rescuing cells whose receptor lost affinity during somatic hypermutation [59] Contrary to the former data, more recent experiments using GFP as a reporter of RAG2 induction have suggested that RAG expression in GCs may be because of the presence of a small percentage of immature RAG-expressing B cells in the spleen and LNs [60] In any case, these immature B cells probably contribute to the immune response and RAG expression

should now be considered a feature of active GCs [61] RAG expression in intrathyroidal GCs was remarkably high, in some cases well above the levels detected in thymus, and probably indicates the high activity of these GCs Our present data do not allow us to establish which of the following two not mutually exclusive alternatives explains the high level of expression of RAG 1) a very active receptor revision and 2) the presence of a high proportion of immature B cells or, in general, of recent bone marrow emigrants We believe that the phenotype of B cells in intrathyroidal LFs and the cloning of B cells/plasma cells bearing high-affinity antibodies to Tg and TPO from these cells favor the first alternative Plausibly, B lymphocytes recruited from blood into intrathyroidal LFs have low-affinity receptors[62] and may require extensive receptor revision to generate high-affinity B cells Interestingly, evidence for over-active receptor revision has been found in human systemic lupus erythematosus (SLE)[63] and, more recently, in ectopic LFs from rheumatoid arthritis synovium [64]

Selective lymphocyte migration into peripheral lymphoid organs is regulated by adhesion molecules and chemokines HEVs are specialized structures that allow rapid and selective lymphocyte trafficking from the blood into the secondary lymphoid tissues Cutaneous lymphocyte-associated antigen (CLA), a HEV addressin, was detected in intrathyroidal small vessels that are morphologically similar to LN HEV Secondary lymphoid tissue chemokine (SLC), a HEV-expressed chemokine that activates lymphocyte integrins, was also detected in intrathyroidal LFs The distribution of HEVs around the intrathyroidal GCs indicates that this process takes place in the thyroid and in the LN In addition to cell recruitment, the formation of LFs requires cytokines and chemokines that provide the signals for tissue organization [65] Among them, SDF-1[66] and BLC act synergistically the former directs the migration of naive B cells to the GC and the latter induces the subsequent exit of activated B cells [67] Responsiveness to SDF-1 seems to be regulated during B lymphocyte activation and correlates with the location of B cells within the secondary lymphoid organ The relatively high level of transcription of these chemokines found by us in intrathyroidal LFs underlines the parallelism between canonical and intrathyroidal LFs, and the high level of activation of the latter We are currently working to determine the cell source of each of these chemokines, and whether the location of their receptors is in accordance with the suggestion that intrathyroidal GCs can organize and perpetuate themselves (MP Armengol, manuscript in preparation)

The major question that arises from this work is whether intrathyroidal LFs containing GCs are involved in pathogenesis It is difficult to answer this question, because the role of the physiological ectopic LFs that appear during the response to infection has not yet been elucidated It is not clear what advantage is obtained by the immune system with the placement of these advanced posts in the target tissue The LFs in areas very rich in antigen and outside the lymphoid tissue might allow a fast expansion of the response, which thus would reach a high level of intensity The recruitment of weakly autoreactive B cells in the thyroid and the extensive revision of the receptors in these cells (which thus would acquire high-affinity surface Igs), may be important for the production of high-affinity autoantibodies In a normal LF, autoreactive B cells would be eliminated by apoptosis as they would encounter soluble antigen[31] but this does not happen to the B cells in intrathyroidal GCs despite the availability of very high levels of antigen, thus suggesting that the microenvironment in ectopic LFs is permissive for autoimmune responses Later, self-antigen presentation by autoreactive B cells and perhaps also by both classical and rogue antigen presenting cells (APCs), such as thyrocytes expressing high levels of histocompatibility leucocyte antigen (HLA) and adhesion molecules[68–70] may be crucial for the maintenance and expansion of the autoimmune response In this scenario it is easy to predict that autoimmune responses would be more difficult to control once LFs with GCs develop in the target tissue

The event that initiates AITD still has to be identified, but sudden changes in the level of iodine intake are probably important [70] It is not difficult to conceive that an initial nonspecific inflammatory response induced by local iodine toxicity could lead to the secretion of inflammatory cytokines and chemokines by macrophages, dendritic cells, and the thyroid epithelial follicular cells themselves In certain circumstances, endothelial cells may acquire the features of HEVs and recruit B and T lymphocytes whereas some stromal cells evolve into follicular dendritic cells In this case, the simultaneous onset of the immune response in the LNs is not so crucial, as the lymphocytes in the thyroid glands could promote the immune response

The possible involvement of intrathyroidal lymphoid tissue in AITD suggests that the local administration of immunosuppressive therapy could control the disease This is not so important in the case of AITD, because the currently available treatment is overall satisfactory, however, it may be important for other tissue-specific autoimmune diseases because the administration of a local treatment would result in side effects that are less severe than systemic immunosuppressive treatment Overall, our results support the relevance of the events in the target organ in the pathogenesis of organ-specific autoimmunity

Acknowledgments

We thank the colleagues cited in the text for their generous donations of antibodies and other reagents (J F Tedder, R Vilella, P Garrone), C Lopez for measuring thyroid autoantibodies, M A Fernandez for his support in microscope image acquisition and processing, Dr A Alastrue, Dr Escalante, and Dr G Obiols for help in collecting thyroid sample materials, Dr L Alcalde, Dr M Sospedra, and Dr F Vargas for help in tissue processing, Pharmacia-Upjohn for preparing and supplying us with biotinylated Tg and TPO antigens, Dr J Verdaguer and M Cullell for critical revision of the manuscript, and to our colleagues in the Endocrine Division and to Prof M Foz for their support and encouragement

References

1 Weetman AP, McGregor AM Autoimmune thyroid disease further developments in our understanding Endocr Rev 1994, 15 788–830
2 Ajjan RA, Kemp EH, Waterman EA, Watson PF, Endo T, Onaya T, Weetman AP Detection of binding and blocking autoantibodies to the human sodium-iodide symporter in patients with autoimmune thyroid disease J Clin Endocrinol Metab 2000, 85 2020–2027
3 Rapoport B, Chazenbalk GD, Jaume JC, McLachlan SM The thyrotropin (TSH) receptor interaction with TSH and autoantibodies Endocr Rev 1998, 19 673–716
4 Fukuma N, Petersen VB, McLachlan SM, Pegg CA, Rees Smith B Human monoclonal thyroglobulin autoantibodies of high affinity I Production, characterisation and interaction with murine monoclonal thyroglobulin antibodies Autoimmunity 1991, 10 291–295
5 Prentice L, Kiso Y, Fukuma N, Horimoto M, Petersen V, Grennan F, Pegg C, Furmaniak J, Rees Smith B Monoclonal thyroglobulin autoantibodies variable region analysis and epitope recognition J Clin Endocrinol Metab 1995, 80 977–986
6 Portolano S, Seto P, Chazenbalk GD, Nagayama Y, McLachlan SM, Rapoport B A human Fab fragment specific for thyroid peroxidase generated by cloning thyroid lymphocyte-derived immunoglobulin genes in a bacteriophage lambda library Biochem Biophys Res Commun 1991, 179 372–377
7 Hexham JM, Furmaniak J, Pegg C, Burton DR, Smith BR Cloning of a human autoimmune response preparation and sequencing of a human anti-thyroglobulin autoantibody using a combinatorial approach Autoimmunity 1992, 12 135–141
8 McIntosh RS, Asghar MS, Watson PF, Kemp EH, Weetman AP Cloning and analysis of IgG kappa and IgG lambda anti-thyroglobulin autoantibodies from a patient with Hashimoto's thyroiditis evidence for in vivo antigen-driven repertoire selection J Immunol 1996 157 927–935
9 Nye L, De Carvalho LP, Roitt IM An investigation of the clonality of human autoimmune thyroglobulin antibodies and their light chains Clin Exp Immunol 1981, 46 161–170
10 Finke R, Seto P, Ruf J, Carayon P, Rapoport B Determination at the molecular level of a B-cell epitope on thyroid peroxidase likely to be associated with autoimmune thyroid disease J Clin Endocrinol Metab 1991, 73 919–921
11 Estienne V, McIntosh RS, Ruf J, Asghar MS, Watson PF, Carayon P, Weetman AP Comparative mapping of cloned human and murine antithyroglobulin antibodies recognition by human antibodies of an immunodominant region Thyroid 1998, 8 643–646
12 Guo J, McIntosh RS, Czarnocka B, Weetman AP, Rapoport B, McLachlan SM Relationship between autoantibody epitopic recognition and immunoglobulin gene usage Clin Exp Immunol 1998, 111 408–414
13 McIntosh R, Watson P, Weetman A Somatic hypermutation in autoimmune thyroid disease Immunol Rev 1998, 162 219–231
14 McLachlan SM, Rapoport B Autoimmune response to the thyroid in humans thyroid peroxidase the common autoantigenic denominator Intern Rev Immunol 2000, 19 587–618
15 Martin A, Barbesino G, Davies TF T cell receptors and autoimmune thyroid disease—signposts for T-cell-antigen driven diseases Int Rev Immunol 1999, 18 111–118
16 Bottazzo GF, Doniach D Autoimmune thyroid disease Annu Rev Med 1986, 37 353–359
17 McLachlan SM, McGregor A, Smith BR, Hall R Thyroid-autoantibody synthesis by Hashimoto thyroid lymphocytes Lancet 1979, 1 162–163
18 McLachlan SM, Fawcett J, Atherton MC, Thompson P, Baylis P, Smith BR Thyroid autoantibody synthesis by cultures of thyroid and peripheral blood lymphocytes II Effect of thyroglobulin on thyroglobulin antibody synthesis Clin Exp Immunol 1983, 52 620–628
19 McLachlan SM, Dickinson A, Baylis P, Proctor S, Rees Smith B Enrichment and depletion of thyroglobulin autoantibody synthesizing lymphocytes Clin Exp Immunol 1983, 53 397–405
20 Atherton MC, McLachlan SM Pegg CA, Dickinson A, Baylis P, Young ET, Proctor SJ, Rees Smith B Thyroid autoantibody synthesis by lymphocytes from different lymphoid organs fractionation of B cells on density gradients Immunology 1985, 55 271–279
21 McLachlan SM, Pegg CA, Atherton MC, Middleton SL, Clark F, Rees Smith B TSH receptor antibody synthesis by thyroid lymphocytes Clin Endocrinol 1986, 24 223–230
22 Randen I, Mellbye OJ, Forre O, Natvig JB The identification of germinal centres and follicular dendritic cell networks in rheumatoid synovial tissue Scand J Immunol 1995, 41 481–486
23 Schröder AE, Greiner A Seyfert C, Berek C Differentiation of B cells in the nonlymphoid tissue of the synovial membrane of patients with rheumatoid arthritis Proc Natl Acad Sci USA 1996, 93 221–225
24 Wagner UG Kurtin PJ, Wahner A, Brackertz M, Berry DJ, Goronzy JJ, Weyand CM The role of CD8+CD40L+ T cells in the formation of germinal centres in rheumatoid synovitis J Immunol 1998, 161 6390–6397
25 Shione H, Fujii Y, Okumura M, Yakeuchi Y, Inoue AM, Matsuda H Failure to down-regulate Bcl-2 protein in thymic germinal center B cells in myasthenia gravis Eur J Immunol 1997, 27 805–809
26 Stott D, Hiepe F, Hummel M, Steinhauser GCB Antigen-driven clonal proliferation of B cell within the target tissue of an autoimmune disease' J Clin Invest 1998, 102 938–943
27 Murakami J, Shimizu Y, Kashii Y, Kato T, Minemura M, Okada K, Nambu S, Takahara T, Higuchi K, Maeda Y, Kumada T, Watanabe A Functional B-cell response in intrahepatic lymphoid follicles in chronic hepatitis C Hepatology 1999 30 143–150
28 Zaitoun AM The prevalence of lymphoid follicles in Helicobacter pylori associated gastritis in patients with ulcers and non-ulcer dyspepsia J Clin Pathol 1995, 48 325–329
29 MacLennan IC Germinal centers Annu Rev Immunol 1994, 12 117–139
30 Liu YJ, Arpin C Germinal center development Immunol Rev 1997, 156 111–126
31 Shokat KM, Goodnow CC Antigen-induced B-cell death and elimination during germinal-centre immune responses Nature 1995, 375 334–338
32 Pulendran B, van Driel R, Nossal GJ Immunological tolerance in germinal centres Immunol Today 1997, 18 27–32
33 Han S, Dillon SR, Zheng B, Shimoda M, Schlissel MS, Kelsoe G V(D)J recombinase activity in a subset of germinal center B lymphocytes Science 1997, 278 301–305
34 Hikida M, Mori M Takai T, Tomochika K, Hamatani K, Ohmori H Reexpression of Rag-1 and Rag-2 genes in activated mature mouse B cells Science 1996, 274 2092–2094
35 Giachino C, Padovan E, Lanzavecchia A Re-expression of RAG-1 and RAG-2 genes and evidence for secondary rearrangements in human germinal center B lymphocytes Eur J Immunol 1998, 28 3506–3513
36 Ludewig B, Odermatt B, Landmann S, Hengartner H, Zinkerngel RM Dendritic cells induce autoimmune diabetes and maintain disease via de novo formation of local lymphoid tissue J Exp Med 1998, 188 1493–1501
37 Falcone M, Lee J, Patstone G, Yeung B, Sarvetnick N B lymphocytes are crucial antigen-presenting cells in the pathogenic autoimmune response to GAD65 antigen in nonobese diabetic mice J Immunol 1998, 161 1163–1168
38 Lucas-Martin A, Foz-Sala M, Todd I, Bottazzo GF, Pujol-Borrell R Occurrence of thyrocyte HLA class II expression in a wide variety of thyroid diseases relationship with lymphocytic infiltration and thyroid autoantibodies J Clin Endocrinol Metab 1988, 66 367–375
39 Sospedra M, Obiols G, Babi LF, Tolosa EF, Vargas F, Roura-Mir C, Lucas-Martin A, Ercilla G, Pujol-Borrell R Hyperinducibility of HLA class II expression of thyroid follicular cells from Graves' disease A primary defect? J Immunol 1995, 154 4213–4222
40 Rose ML, Birbeck MSC, Wallis VJ, Forrester GA, Davies AJS Peanut lectin binding properties of germinal centres of mouse lymphoid tissue Nature 1980, 364–366
41 Sospedra M, Tolosa E, Armengol P, Ashhab Y, Urlinger S, Lucas-Martin A Foz-Sala M, Jaraquemada D, Pujol-Borrell R Hyperexpression of transporter in antigen processing-1 (TAP-1) in thyroid glands affected by autoimmunity a contributing factor to the breach of tolerance to thyroid antigens? Clin Exp Immunol 1997, 109 98–106
42 Foy TM, Laman JD, Ledbetter JA, Aruffo A, Claassen E, Noelle RJ gp39-CD40 interactions are essential for germinal center formation and the development of B cell memory J Exp Med 1994, 180 157–163
43 Grammer AC, McFarland RD, Heaney J, Darnell BF, Lipsky PE

Expression, regulation, and function of B cell-expressed CD154 in germinal centers J Immunol 1999, 163 4150–4159
44 Giordano C, Stassi G, De Maria R, Todaro M, Richiusa P, Papoff G, Ruberti G, Bagnasco M, Testi R, Galluzzo A Potential involvement of Fas and its ligand in the pathogenesis of Hashimoto's thyroiditis Science 1997, 275 960–963
45 Terol MJ, Cid MC, Lopez-Guillermo A, Juan M, Yague J, Miralles A, Vilella R, Vives J, Cardesa A, Montserrat E, Campo E Expression of intercellular adhesion molecule-3 (ICAM-3/CD50) in malignant lymphoproliferative disorders and solid tumors Tissue Antigens 1996, 48 271–277
46 Tu L, Delahunty MD, Ding H, Luscinskas FW, Tedder TF The cutaneous lymphocyte antigen is an essential component of the L-selectin ligand induced on human vascular endothelial cells J Exp Med 1999, 189 241–252
47 Kofler R, Wick G Immunofluorescence localization of thyroglobulin-autoantibody producing cells in various organs of obese strain (OS) chickens Z Immunol Forsch 1978, 154 88–93
48 Ratanachaiyavong SM, McGregor AM Immunosuppressive effects of antithyroid drugs Clin Endocrinol Metab 1985, 14 449–466
49 Pellegriti G, Belfiore A, Giuffrida D, Lupo L, Vigneri R Outcome of differentiated thyroid cancer in Grave's patients J Clin Endocrinol Metab 1998, 83 2805–2809
50 Tew JG, Phipps RP, Mandel TE The maintenance and regulation of the humoral immune response persisting antigen and the role of follicular antigen-binding dendritic cells as accessory cells Immunol Rev 1980, 53 175–201
51 Perry M, Whyte A Immunology of the tonsils Immunol Today 1998 19 414–421
52 Hykek E, Isaacson PG Primary B cell lymphoma of the thyroid and relationship to Hashimoto thyroiditis Hum Pathol 1988, 9 1315–1326
53 Williams ED Malignant lymphoma of the thyroid Clin Endocrinol Metab 1991, 10 379–389
54 Kiljanski J, Nebes V, Stachura I, Kennerdell JS, Wall JR Should Graves' disease be considered a collagen disorder of the thyroid, skeletal muscle and connective tissue? Horm Metab Res 1995, 27 528–532
55 Nemazee D Receptor selection in B and T lymphocytes Annu Rev Immunol 2000, 18 19–51
56 Han S, Zheng B, Schatz DG, Spanopoulou E, Kelsoe G Neoteny in lymphocytes Rag-1 and Rag-2 expression in germinal center B cells Science 1996, 374 2094–2097
57 Papavasiliou F, Casellas R, Suh H, Qin XF, Besmer E, Pelanda R, Nemazee D, Rajewsky K, Nussenzweig MC V(D)J recombination in mature B cells a mechanism for altering antibody responses Science 1997, 278 298–301
58 Hikida M, Ohmori H Rearrangement of lambda light chain genes in mature B cells in vitro and in vivo Function of reexpressed recombination-activating gene (RAG) products J Exp Med 1998, 187 795–799
59 Meffre E, Papavasiliou F, Cohen P, de Bouteiller O, Bell D, Karasuyama H, Schiff C, Banchereau J, Liu YJ, Nussenzweig MC Antigen receptor engagement turns off the V(D)J recombination machinery in human tonsil B cells J Exp Med 1998, 188 765–772
60 Yu W, Nagaoka H, Jankovic M, Misulovin Z, Suh H, Rolink A, Melchers F, Meffre E, Nussenzweig MC Continued RAG expression in late stages of B cell development and no apparent re-induction after immunization Nature 1999, 400 682–687
61 Monroe RJ, Seidl KJ, Gaertner F, Han S, Chen F, Sekiguchi J, Wang J, Ferrini R, Davidson L, Kelsoe G, Alt FW RAG2 GFP knockin mice reveal novel aspects of RAG2 expression in primary and peripheral lymphoid tissues Immunity 1999, 11 201–212
62 Sospedra M, Ferrer-Francesch X, Dominguez O, Juan M, Foz-Sala M, Pujol-Borrell R Transcription of a broad range of self-antigens in human thymus suggests a role for central mechanisms in tolerance toward peripheral antigens J Immunol 1998, 161 5918–5929
63 Dorner T, Foster SJ, Farner NL, Lipsky PE Immunoglobulin kappa chain receptor editing in systemic lupus erythematosus J Clin Invest 1998, 102 688–694
64 Itoh K, Meffre E, Albesiano E, Farber A, Dines D, Stein P, Asnis SE, Furie RA, Jain RI, Chiorazzi N Immunoglobulin heavy chain variable region gene replacement as a mechanism for receptor revision in rheumatoid arthritis synovial tissue B lymphocytes J Exp Med 2000, 192 1151–1164
65 Ansel KM, Ngo VN, Hyman PL, Luther SA, Forster R, Sedgwick JD, Browning JL, Lipp M, Cyster JG A chemokine-driven positive feedback loop organizes lymphoid follicles Nature 2000, 406 309–314
66 Bleul CC, Schultze JL, Springer TA B lymphocyte chemotaxis regulated in association with microanatomic localisation, differentiation state, and B cell receptor engagement J Exp Med 1998, 187 753–762
67 Gunn M, N'go VN, Ansel KM, Ekland EH, Jason GC, Williams LT A B cell homing chemokine made in lymphoid follicles activates Burkitt's lymphoma receptor-1 Nature 1998, 391 799–803
68 Pujol-Borrell R, Hanafusa T, Chiovato L, Bottazzo GF Lectin-induced expression of DR antigen on human cultured follicular thyroid cells Nature 1983, 303 71–73
69 Bottazzo GF, Pujol-Borrell R, Hanafusa TMF Role of aberrant HLA-DR expression and antigen presentation in induction of endocrine autoimmunity Lancet 1983, 2 1115–1118
70 Verma S, Hutchings P, Guo J, McLachlan S, Rapoport B, Cooke A Role of MHC class I expression and CD8(+) T cells in the evolution of iodine-induced thyroiditis in NOD-H2(h4) and NOD mice Eur J Immunol 2000, 30 1191–1202

Chemokines Determine Local Lymphoneogenesis and a Reduction of Circulating CXCR4$^+$ T and CCR7 B and T Lymphocytes in Thyroid Autoimmune Diseases[1]

Maria-Pilar Armengol,* Cristina B. Cardoso-Schmidt,* Marco Fernández,† Xavier Ferrer,* Ricardo Pujol-Borrell,[2]* and Manel Juan*

Chemokines and their corresponding receptors are crucial for the recruitment of lymphocytes into the lymphoid organs and for its organization acting in a multistep process. Tissues affected by autoimmune disease often contain ectopic lymphoid follicles which, in the case of autoimmune thyroid disorders, are highly active and specific for thyroid Ags although its pathogenic role remains unclear. To understand the genesis of these lymphoid follicles, the expression of relevant cytokines and chemokines was assessed by real time PCR, immunohistochemistry and by in vitro assays in autoimmune and nonautoimmune thyroid glands. Lymphotoxin α, lymphotoxin β, C-C chemokine ligand (CCL) 21, CXC chemokine ligand (CXCL) 12, CXCL13, and CCL22 were increased in thyroids from autoimmune patients, whereas CXCL12, CXCL13, and CCL22 levels were significantly higher in autoimmune glands with ectopic secondary lymphoid follicles than in those without follicles. Interestingly, thyroid epithelium produced CXCL12 in response to proinflammatory cytokines providing a possible clue for the understanding of how tissue stress may lead to ectopic follicle formation. The finding of a correlation between chemokines and thyroid autoantibodies further suggests that intrathyroidal germinal centers play a significant role in the autoimmune response. Unexpectedly, the percentage of circulating CXCR4$^+$ T cells and CCR7$^+$ B and T cells (but not of CXCR5) was significantly reduced in PBMCs of patients with autoimmune thyroid disease when they were compared with their intrathyroidal lymphocytes. This systemic effect of active intrathyroidal lymphoid tissue emerges as a possible new marker of thyroid autoimmune disease activity. ***The Journal of Immunology,*** **2003, 170: 6320–6328.**

Antigens reach the lymph node transported by dendritic cells (DCs),[3] which perform an initial selection of potentially dangerous Ags via pattern recognition receptors (1–3) In the secondary lymphoid organs, these Ags are presented to T cells with a repertoire that has already been purged from self-reacting cells before leaving the thymus Naive T cells recirculate only through the secondary lymphoid tissue, thus reducing the chances of these cells interacting with peripheral self-Ags (4) Lymph nodes are organized to favor the encounter between foreign Ags and lymphocytes bearing complementary receptors and also to facilitate crucial interactions between B and T cells on encounter with Ag Within the lymph nodes, lymphoid follicles (LFs) are complex small structures in which many crucial processes take place such as somatic hypermutation, affinity maturation, isotype switch (5), and receptor revision In the germinal centers (GCs), autoreactive B cells are presumably generated de novo, thus requiring specific mechanisms to maintain tolerance (6) LFs not only develop within the secondary lymphoid tissues, but also they sometimes form within the parenchyma of nonlymphoid organs when the immune response fails to eradicate an infectious agent (7), e g , hepatitis C (8) or *Helicobacter pylori* gastritis (9), and in autoimmunity Fully developed ectopic LFs are also found in several autoimmune diseases such as autoimmune thyroiditis (10), rheumatoid arthritis (11, 12), myasthenia gravis (13, 14), Sjogren's disease (15), and cryptogenic fibrosing alveolitis (16) It has been suggested that ectopic lymphoid tissue constitutes a different compartment of the lymphoid system that should be called the tertiary lymphoid tissue (TLT) (17), but its specific functions have not been fully elucidated yet

Hashimoto's disease (HT) and Graves-Basedow thyrotoxicosis (GD) are two clinical forms of autoimmune thyroid disease (AITD) (18) in which lymphoid infiltration commonly evolves into secondary LFs (19) Despite longtime suspicion (20), only recently it has been shown that these structures are fully functional, yet their role in pathogenesis is unclear (19) To sustain their activity, intrathyroidal LFs must be included in the migration circuits of B and T lymphocytes However, migration by itself is not sufficient, because massive infiltration can occur in the thyroid without LF neogenesis Different types of organizing factors must be present in the tissue It is currently accepted that lymphotoxin (LT) α, LTβ, C-C chemokine ligand (CCL) 21 (secondary lymphoid tissue chemokine), CXC chemokine ligand (CXCL) 12 (stromal cell-derived factor-1), CXCL13 (B cell-attracting chemokine-1), and

*Laboratory of Immunobiology for Research and Application to Diagnosis, Center for Transfusion and Tissue Bank, Badalona, Spain, and †Cytometry Unit, Hospital Universitari "Germans Trias i Pujol," Department of Cell Biology, Physiology, and Immunology, Universitat Autònoma de Barcelona, Barcelona, Spain

Received for publication December 20, 2002 Accepted for publication March 27, 2003

The costs of publication of this article were defrayed in part by the payment of page charges This article must therefore be hereby marked *advertisement* in accordance with 18 U S C Section 1734 solely to indicate this fact

[1] This work was supported by Projects 99/1063 and 01/1110 from the "Fondo de Investigaciones Sanitarias" (to M P A) and by a grant from the Ministerio de Educación y Cultura (to C B C -S)

[2] Address correspondence and reprint requests to Dr R Pujol-Borrell, Laboratory of Immunobiology for Research and Application to Diagnosis Immunology Unit, Hospital Universitari 'Germans Trias i Pujol," Ctra Canyet s/n, 08916 Badalona (Barcelona), Spain E mail address ricardo pujol@ub es

[3] Abbreviations used in this paper DC, dendritic cell, LF, lymphoid follicle, CCL, C C chemokine ligand, CXCL, CXC chemokine ligand, LT, lymphotoxin, GC, germinal center, HT, Hashimoto's disease, GD, Graves Basedow thyrotoxicosis, TLT, tertiary lymphoid tissue, AITD, autoimmune thyroid disease, MNG, multinodular goiter, TPO, thyroid peroxidase, PT, palatine tonsils, ITLs, intrathyroidal lymphocytes, rh, recombinant human

0022-1767/03/$02 00

CCL22 (macrophage-derived chemokine) are probably the most important mediators for GC formation (21) CCL21 selectively attracts naive lymphocytes and DCs via CCR7 (CD197) (22), and DCs in turn produce CCL22 that induces segregation of lymphocytes into T and B zones (23) CXCL12 has homeostatic chemotactic activity via CXCR4 (CD184) on most T and B cells subpopulations and contributes decisively to the development of GCs and maintenance of LFs (24) CXCL13 organizes the distribution of B and T cells within the GCs via CXCR5 (25)

In previous studies, CCL3 (macrophage-inhibitory protein-1α), CCL4 (macrophage-inhibitory protein-1β), CCL5 (26), CCL21, CXCL12, and CXCL13 (19) have been detected in AITD glands and elevated levels of macrophage chemoattractant protein-1 in the patient's sera (27), whereas CXCR3 and CCR5 (28) were associated with GD In contrast, in experimental autoimmune thyroiditis (29), several chemokines have been involved in the disease There are no systematic studies on the expression of the chemokines responsible for the GC organization and their corresponding receptors in AITD.

We report here that autoimmune thyroid glands hyperexpress LTα, IFN-γ, CXCL12, CXCL13, and CCL22 Those containing secondary lymphoid follicles overexpress IFN-γ, CXCL12, CXCL13, and CCL22 and express LTβ and CCL21, and the corresponding receptors CXCR4, CXCR5, LTβR, and CCR7. We found that thyroid epithelial cells produce CXCL12 in vivo and in vitro, this may explain the relatively high frequency of LFs in thyroid glands In patients with intrathyroidal LFs, which are rich in CXCR4$^+$ T lymphocytes, we detected a concomitant reduction in circulating CXCR4$^+$ T cells and also in CCR7$^+$ T and B lymphocytes This constitutes an unexpected effect on the periphery of intrathyroidal lymphoid neogenesis and suggests the existence of a general disturbance in lymphocyte recirculation circuit as part of AITD

Materials and Methods

Tissues and cell culture

Thyroid tissue was obtained from 34 patients (27 of them had been included in a previous study (19)) 4 HT, 12 GD with LFs, 11 GD without LFs, 1 multinodular goiter (MNG) with thyroiditis, 4 MNGs and 2 multiorgan donor glands MNG and donor glands were used as nonautoimmune thyroid controls Clinical diagnosis was made based on usual thyroid tests and confirmed by histopathology Thyroid peroxidase (TPO) and thyroglobulin Abs were measured by ELISA (Immunowell, San Diego, CA), and anti-thyroid-stimulating hormone receptor Abs were measured by RIA (Brahms Diagnostica, Berlin, Germany) (Table I) A human thymus, two palatine tonsils (PT), and two lymph nodes (one of them from the HT385 patient) were used as reference lymphoid tissue Because the palatine tonsils were not inflamed at the time of surgery, we considered their values basal Cervical lymph nodes containing highly active lymphoid follicles were considered positive controls For molecular biology techniques and intrathyroidal lymphoid follicle staining, 4-μm cryosections from thyroids (3 of 4 HTs, 16 of 23 GDs, 4 of 5 MNGs, and 2 of 2 normal donors) and tissue controls were used

Adherent cells (95–98% thyrocytes) were separated from intrathyroidal lymphocytes (ITLs) after thyroid gland digestion (30) by overnight seeding To avoid culture chemokine receptor modulation, ITLs were separated by density gradient from thyrocytes immediately after digestion The lymphocyte-thyroid follicular cell ratio was assessed by flow cytometry, using this value for correlation analysis

Thyroid monolayers were maintained in RPMI containing 10% FCS, and the percentage of FCS was decreased to 2% 2 h before exposure to the cytokines recombinant human (rh) IL-1β 200 IU/ml (DAKO, Glostrup, Denmark), rhIFN-γ 500 IU/ml, or rhTNF-α 500 IU/ml (supplied by G R Adolph, Boehringer Institute, Vienna, Austria) The human thyroid cell line HT93 was also used It was generated by transfection with a SV40 early region construct and originally produced thyroglobulin (31) It has maintained epithelial features, and we have already used it in studies of HLA regulation

Table I *Thyroid samples used*

Sample	Anti-Tg[a] (IU/ml)	Anti-TPO (IU/ml)	Anti-TSHR (IU/L)	% LI	ILFs
GD1	–	–	80 0	ND	+
GD2	598 0	1155 0	67 0	70 2	+
GD3	ND	ND	28	38 0	+
GD4	–	–	16 0	ND	+
GD5	–	ND	33	11 1	+
GD6	–	46	10 1	10 6	+
GD7	70	53	15 5	10 2	–
GD8	–	25	20	ND	–
GD9	–	–	–	3 02	–
GD10	172 1	39 2	178 0	27 7	+
GD11	–	–	–	1 2	–
GD12	–	–	1 14	38 9	+
GD13	190	1001	14 9	ND	+
GD14	1265	1001	85 9	45 4	+
GD15	–	550 0	–	38 8	+
GD16	–	120	>40	89 3	+
GD17	–	28	4 0	11 4	+
GD18	–	–	4 1	54 5	–
HT1	774 0	105,000	–	76 6	+
HT2	ND	ND	ND	66 6	+
HT3	ND	ND	ND	80 2	+
HT4	–	85 1	–	60 2	+
MNG1	–	45 9	1 2	21 7	+
MNG2	–	–	–	2 0	–
MNG3	–	–	1 6	6 1	–
MNG4	–	37 9	1 4	3 5	–
MNG5	–	–	–	5 2	–
MNG6	–	–	–	11 7	–
HD1	–	–	–	3 5	–
HD2	–	–	–	1 2	–

[a] Tg, Thyroglobulin, TSHR, thyroid stimulating hormone receptor, LI, lymphocytic infiltration, ILFs, intrathyroidal lymphoid follicles, –, negative

PBMCs from 12 patients (obtained at the same time as the thyroid resection procedure) and 12 healthy donors were separated using a Ficoll (Sigma-Aldrich, St Louis, MO) discontinuous density gradient

Immunofluorescent histochemistry and FACS

Sources of Abs were goat Abs to CXCL12, CCL21 and CXCL13, and murine mAbs to CXCR4 and CXCR5 from R&D Systems (Minneapolis, MN), mAb to cytokeratin 8–18 from Novocastra Laboratories (Newcastle upon Tyne, U K), mAb to CD83 from T F Tedder (Duke University Medical Center, Durham, NC), mAbs to human CD19, CD20, CD3, and CD5 from R Vilella (Hospital Clínic Barcelona, Barcelona, Spain), murine mAb to CD21L from P Garrone (Laboratory for Immunological Research, Schering-Plough, Paris, France), mAb to CD4 and CD8 from M Bofill (Fundcaó IRSI-Caixa, London, U K), mAbs to CD3-PerCP, CCR7, CD45RA-FITC, and CD45RO-PE from BD PharMingen (San Diego, CA), and mAb to CD19-PECy5 from DAKO, and fluorochrome-labeled secondary Abs from Southern Biotechnology (Birmingham, AL) For thyroperoxidase detection, a high titer anti-TPO-positive human serum was used

Cryosections were fixed in 4% paraformaldehyde (CXCL12 and CXCL13), or cold acetone (CCL21) Independent observers blindly examined slides Images were acquired with a high resolution video camera and analyzed using Openlab software (Improvision, Coventry, U K)

Three-color flow cytometry was performed using a FACScan (BD Biosciences, San Jose, CA) to assess chemokine receptors expression in ITLs and PBMCs Data were acquired and analyzed with the CellQuest software (BD Biosciences) Intrathyroidal T and B cells were sorted in a FACSVantage cell sorter (BD Biosciences), their purity ranged from 94 to 99%

CXCL12 ELISA

CXCL12 levels were measured in supernatants from HT93 cells and from thyroidal cultures by an in-house sandwich ELISA (T Gallart, Hospital Clínic Barcelona, Barcelona, Spain) Plates containing 96 wells were coated with Abs to human CXCL12α (R&D Systems) Soluble CXCL12α was detected with a biotinylated Ab to human CXCL12α, followed by streptavidin peroxidase incubation The ELISA detection range was 0 39–200 ng/ml (human CXCL12α, PeproTech, Rocky Hill, NJ)

Table II *Primers, probes, and conditions used to amplify/hybridize cytokines/chemokines using semiquantitative and real time PCR*

	Primers and Oligoprobes	Semiquantitative PCR	Real Time PCR
GAPDH	Sense 5′-TCTTCTTTTGCGTCGCCAG-3′ Antisense 5′-AGCCCCAGCCTTCTCCA-3′	95°C 7 min + 28 × (95°C 20 s/68°C 15 s/72°C 15 s) + 72°C 10 min	95°C 6 s + 35 × (94°C 15 s/63°C 10 s/72°C 15 s) + 63–95°C
LTα	Sense 5′-ACGGCGATGCGGCTGATG-3′ Antisense 5′-ACTGACCCACGGCTCCAC-3′ Probe 5′-GGCGATGCGGCTGATGGT-3′	95°C 7 min + 30 × (94°C 30 s/70°C 15 s/72°C 40 s) + 72°C 7 min	ND
LTβ	Sense 5′-ATTACCCACCTCTCACCTCTCCCCT-3′ Antisense 5′-GCTGTTCTATCCCCTTCCATTCTCT-3′ Probe 5′-CCAGCCCAGCCCCCA-3′	95°C 7 min + 30 × (94°C 30 s/68°C 15 s/72°C 25 s) + 72°C 7 min	ND
LTβR	Sense 5′-GGTGCCTCCGTGTGCGTC-3′ Antisense 5′-GGGGACGCAGTGGTTGTT-3′ Probe 5′-TTTTCCTGGTCCCTTGCA-3′	95°C 7 min + 28 × (95°C 20 s/68°C 15 s/72°C 15 s) + 72°C 10 min	ND
IFN-γ	Sense 5′-GTTTTGGGTTCTCTTGG-3′ Antisense 5′-ATTACTGGGATGCTCTT-3′ Probe 5′-GGGAAGCGAAAAAGGAGTCA-3′	95°C 7 min + 30 × (94°C 30 s/60°C 15 s/72°C 20 s) + 72°C 7 min	ND
CXCL12	Sense 5′-GTCGTGGTCGTGCTGGTC-3′ Antisense 5′-CGGGCTACAATCTGCAGG-3′ Probe 5′-TGCCTCAGCGACGGG-3′	95°C 7 min + 30 × (95°C 20 s/68°C 15 s/72°C 15 s) + 72°C 10 min	95°C 6 s + 35 × (94°C 15 s/60°C 7 s/72°C 10 s) + 65–95°C
CCL21	Sense 5′-AAGGCAGTGATGGAGGGG-3′ Antisense 5′-CTGGGCTGGTTTCTGTGG-3′ Probe 5′-CTTGGTTCCTGCTTCCG-3′	95°C 7 min + 35 × (95°C 20 s/68°C 15 s/72°C 15 s) + 72°C 10 min	95°C 6 s + 45 × (94°C 15 s/63°C 10 s/72°C 10 s) + 68–95°C
CXCL13	Sense 5′-CGACATCTCTGCTTCTC-3′ Antisense 5′-ACTTCCATCATTCTTTG-3′ Probe 5′-ACAACCATTCCCACGG-3′	95°C 7 min + 35 × (95°C 20 s/68°C 15 s/72°C 15 s) + 72°C 10 min	95°C 6 s + 45 × (94°C 15 s/52°C 7 s/72°C 15 s) + 60–95°C
CCL22	Sense 5′-GAGACATACAGGACAGAGCATGGAT-3′ Antisense 5′-ATGGAGATCAGGGAATGCAGAGAG-3′	95°C 7 min + 30 × (95°C 20 s/68°C 15 s/72°C 15 s) + 72°C 10 min	95°C 6 s + 40 × (95°C 10 s/68°C 5 s/72°C 18 s) + 63–95°C

RT-PCR and quantitative real time PCR

RNA was obtained using a modified Chomczynski method (32); genomic DNA was removed and then was retrotranscribed with oligo(dT)$_{15}$ (Pharmacia Biotech, Peapack, NJ) and SuperScript-II (Pharmacia Biotech). cDNA duplicates were amplified by semiquantitative PCR using DynaZyme II (Finnzymes OY, Helsinki, Finland) and specific primers for LTα, LTβ, LTβR, and IFN-γ (conditions listed in Table II). Amplimers were hybridized with [γ-^{32}P]ATP oligoprobes and quantified in a Bio-Rad Molecular Imager-FX (Bio-Rad, Hercules, CA) by using Quantity-One. Results were normalized by GAPDH expression.

For real time PCR, standards and controls for CCL21, CXCL12, CXCL13, and CCL22 were obtained by PCR from thymus, PT, and PHA-stimulated PBMC cDNAs. Amplification products from conventional PCR were quantified in serial dilutions from 10^1 to 10^7 molecules. Real time PCR were performed in a LightCycler (Roche, Mannheim, Germany) using the master mix containing 4 mM $MgCl_2$, 0.5–0.3 μM primers, and 1 μl LightCycler Fast Start DNA Master SYBR Green I (Roche) (the experimental run protocols are described in Table II). The amount of cDNA was calculated by the second derivative method after confirming the specificity of the amplification with the melting curve profiles. The samples and standards were run four times for chemokines/cytokines and six times for GAPDH in nondependent runs. The relative abundance of each chemokine was calculated by normalizing the mean of mRNA sample copies ($mean_{CHEM\text{-}Sample}$) with the corresponding GAPDH one ($mean_{GAPDH\text{-}Sample}$), referred to average levels of PTs, and expressed in arbitrary units (Fig. 1) by the formula $Index_{Sample} = [(Mean_{CHEM\text{-}Sample} \times mean_{GAPDH\text{-}PTs})/(mean_{GAPDH\text{-}Sample} \times mean_{CHEM\text{-}PTs})]$.

Chemotaxis

The transmigration assay was conducted on Transwell plates (5-μm pore size; Corning, Corning, NY), by triplicate or duplicate, depending on cell availability: 3×10^4–10^5 sorted CD3$^+$ and CD19$^+$ cells were plated in the upper chamber; and the lower chamber was filled with medium containing 10–1000 ng/ml human CXCL12 (R&D Systems). Supernatants from thyrocytes cultured with IL-1β, IFN-γ, or TNF-α (at 200, 500, and 500 IU/ml, respectively) taken at peak CXCL12 protein (quantified by the previous ELISA) or control medium were also used to measure spontaneous migration. In some experiments, cells were preincubated with blocking anti-CXCR4 (12G5, 20 μg/ml). Migrated cells were counted using Flow-Count Fluorospheres (Coulter, Miami, FL).

Statistical analysis

Pearson's correlation coefficient, together with parametric (Student *t* test) and nonparametric (Mann-Whitney) tests, were applied to normal and non-normal distributed data, respectively, using the SPSS software package (Microsoft, Seattle, WA). A level of significance of 5% was used in all the statistical evaluations.

Results

LTα, IFN-γ, CXCL12, CXCL13, and CCL22, but not LTβ or LTβR, are overexpressed in autoimmune thyroid glands

The levels of chemokine transcription were analyzed in relation to the diagnosis and presence of intrathyroidal GCs. LTα, IFN-γ,

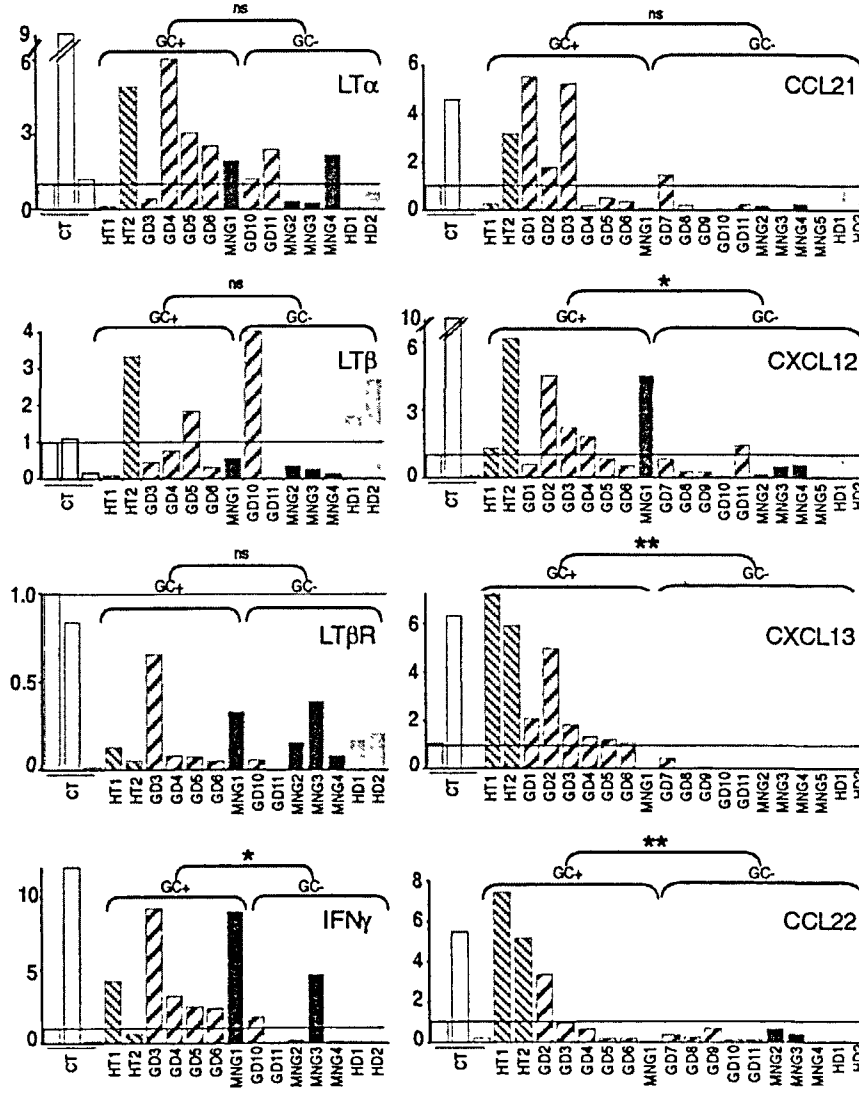

FIGURE 1. mRNA expression of cytokines (LTα, LTβ, LTβR, and IFN-γ) and chemokines (CCL21, CXCL12, CXCL13 and CCL22) in thyroid glands. Expression levels are represented as an index (*y*-axis) referred to the cytokine/chemokine expression in palatine tonsils (this level is given as index = 1 and indicated as a horizontal bar in each graph). The samples are identified with the same code as in Table I: CT, Control tissues (including palatine tonsils, lymph nodes, and purified thyroid follicular cells); HT, Hashimoto's glands; GD, GD glands; MNG, MNG glands; HD, healthy donor glands. GC+, Thyroid glands with visible GCs; GC−, thyroid glands with no visible germinal centers. *, $p < 0.05$; **, $p < 0.01$; ns, nonsignificant.

CXCL12, and CCL22 mRNA levels were higher in AITD glands than in nonautoimmune glands ($p = 0.022$, $p = 0.024$, $p = 0.030$, $p = 0.010$, respectively). Elevated CXCL13 was a constant and exclusive feature of AITD glands ($p < 0.01$) whereas CCL21 showed a nonstatistically significant association with disease ($p = 0.09$). Presence of GC was associated to higher levels of CXCL12, CXCL13, CCL22, and IFN-γ ($n = 20$; $p = 0.022$, $p < 0.001$, $p = 0.007$, and $p = 0.024$, respectively). Lymphocytic infiltration was also associated with CXCL13 and CCL22 levels (CXCL13, $r = 0.972$, $p < 0.0009$; CCL22, $r = 0.983$, $p < 0.0009$). Finally, expression of LTβ and/or of LTβR did not bear a clear relation to diagnosis ($p = 0.6$ and $p = 0.54$) (Fig. 1).

The immunohistochemistry tests showed CCL21$^+$ cells around the GCs in up to 30% of capillaries with features of high endothelial venules (CLA$^+$; Fig. 2). CXCL12 was found in thyroid epithelium (TPO$^+$ and cytokeratin$^+$; Fig. 2) and also in clusters of nonidentified cells amid the lymphocytic infiltration. By contrast, CXCL13$^+$ cells were distributed in the mantle zone of LFs. Although we were unable to clearly identify CD83$^+$ mature DCs or follicular DCs as CXCL13$^+$ producers (due to nonappropriate reagents), the pattern of staining points to the former as the CXCL13 source (Fig. 2).

Thyrocytes are the source of CXCL12

Because production of CXCL12 by thyrocytes has pathogenic implications, we tested the effects of stimuli (IL1β, IFN-γ, or TNF-α) presumably acting in vivo on primary thyroid cell cultures. These cytokines clearly induced a raise of CXCL12α secretion (peak at 6 h) over baseline levels more marked for IL-1β, which produced a 2-fold increase: 7.56 ± 0.75 vs 3.72 ± 1.4 ng/ml (Fig. 3*A*). To rule out the possibility that CXCL12α was derived from contaminating macrophages or fibroblasts, it was also measured in the supernatants of HT93 cells, and similar results were obtained (Fig. 3*A*). Semiquantitative RT-PCR and hybridization detected CXCL12 mRNA in both tissues, confirming ELISA results (Fig. 3*A*). Interestingly, these supernatants from cytokine-stimulated thyrocytes showed a chemotactic activity that was proportional to CXCL12 levels, and chemotaxis was blocked with anti-CXCR4 Abs (Fig. 3*B*).

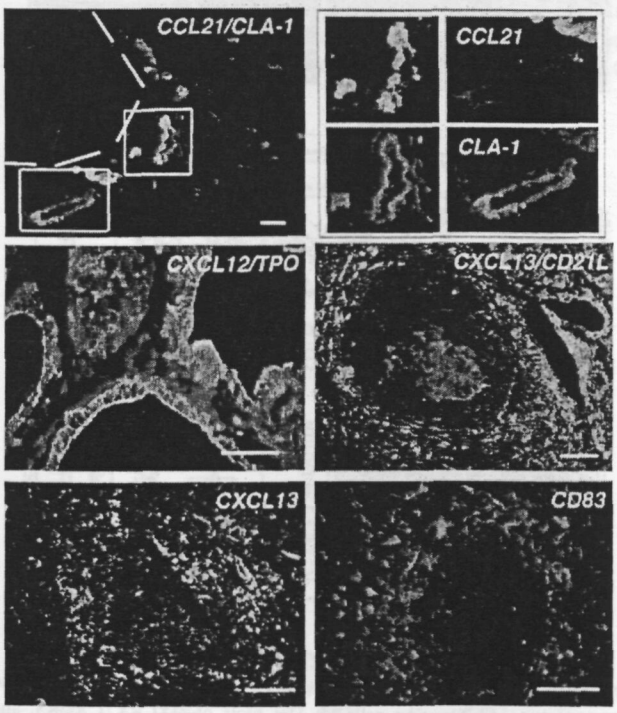

FIGURE 2. Chemokine expression in autoimmune thyroids. Upper left panel, Double immunofluorescent staining of endothelial cells with anti-CCL21 (green) and anti-CLA-1 (red) around the lymphoid follicle (dashed yellow line). Upper right panel, Amplified insets of the previous panel; middle left panel, results of a double exposure for CXCL12 (green) in formalin-fixed sections from GD patients colocalizing with epithelial cells, detected as TPO$^+$ (red); middle right panel, superimposed images of follicular DCs stained using anti-CD21L (red) and with anti-CXCL13 (green); lower left and right panels, nonconsecutive sections stained with anti-CXCL13 (green) and anti-CD83$^+$ (red) show a similar reticular staining pattern and distribution. Image sizes, referred to 100 μm, are represented as yellow lines inside the panels.

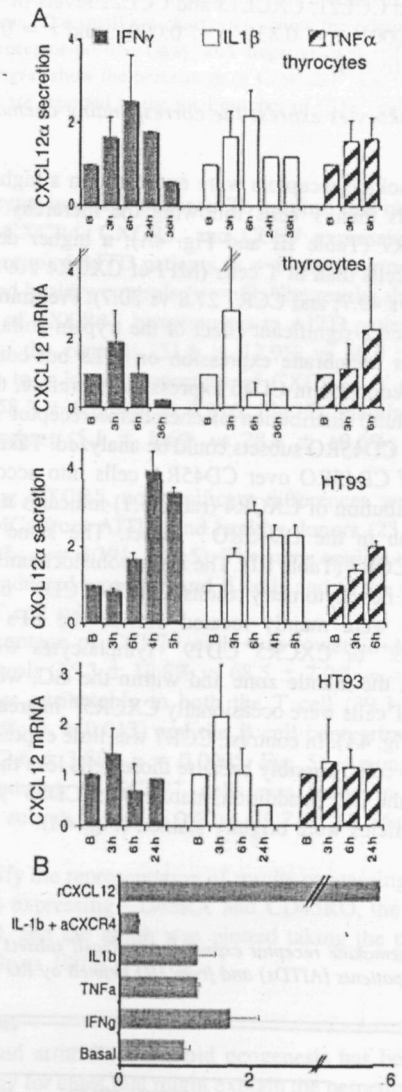

FIGURE 3. Regulation of CXCL12 expression in thyrocytes and its chemotactic activity. *A*, CXCL12 secretion and mRNA expression in thyroid follicular cells and in the HT93 thyroid-derived cell line in baseline conditions (*B*) and after cytokine stimulation. Results are expressed as an index referred to the baseline conditions (index = 1) from four different thyroid glands. *B*, Chemotaxis of PBMCs from healthy donors using supernatants from the aforementioned stimulated thyrocytes (*y*-axis stimuli: IL1β + aCXCR4, supernatant from thyrocytes stimulated with IL-1β and blocked with anti-CXCR4 Ab; IFN-γ, supernatant from thyrocytes stimulated with IFN-γ; TNF-α, supernatant from thyrocytes stimulated with TNF-α). The migration results of a representative experiment are expressed as an index (*x*-axis) and calculated as the ratio between the numbers of migrating cells in the sample and the spontaneous migration.

Because CCL21 and CXCL13 were not detected by PCR in thyrocytes (either in baseline conditions or after stimulation), no further secretion studies were undertaken.

Thyroid autoantibody levels correlate with CXCL13 and CCL22

In a previous study, we reported the association between thyroid autoantibody titers and the presence of intrathyroidal GCs. Here, we describe a correlation between thyroid autoantibody titers and chemokine levels: anti-thyroglobulin Abs correlated with CXCL13 ($r = 0.951$, $p < 0.0001$) and CCL22 ($r = 0.906$, $p < 0.0001$) levels; anti-TPO Abs correlated with CXCL13 ($r = 0.940$, $p < 0.0001$) and CCL22 ($r = 0.910$, $p < 0.0001$) levels. When GD were analyzed vs nonautoimmune glands, anti-thyroid-stimulating hormone receptor Abs correlated with IFN-γ ($n = 14$, $r = 0.726$, $p = 0.025$) and CCL21, CXCL13 and CCL22 levels ($n = 18$; $r = 0.829$, $p < 0.0001$; $r = 0.831$, $p < 0.0001$; and $r = 0.877$, $p < 0.0001$, respectively).

Infiltrating leukocytes express the corresponding chemokine receptors

In ITLs, chemokine receptors were expressed in a higher proportion of B cells than T cells following the hierarchy CXCR4> CXCR5>CCR7 (Table III and Fig. 4*A*); a higher density was reached in B cells than in T cells (MFI of CXCR4 109.9 vs 38.2; CXCR5 140 vs 49.7; and CCR7 27.8 vs 20.7). Preliminary experiments excluded a significant effect of the trypsin-collagenase solution on their membrane expression on ITLs but confirmed an overall 30% reduction in CD45 expression; therefore, the relative (but not absolute) distribution of chemokine receptor among the CD45RA and CD45RO subsets could be analyzed. Taking the predominance of CD45RO over CD45RA cells into account (ratio, 4:3), the distribution of CXCR4 (ratio, 3:1) indicates its preferential expression in the CD45RO$^+$ subset. The same applies to CXCR5 and CCR7 (Table III). The immunohistochemistry studies confirmed the flow cytometry results: CXCR4$^+$CD3$^+$ or CXCR4$^+$CD19$^+$ cells were mainly located outside the LFs (Fig. 4*A*), CXCR5$^+$CD3$^+$ or CXCR5$^+$CD19$^+$ lymphocytes were mainly distributed in the mantle zone and within the GC, whereas only some CD4$^+$ T cells were occasionally CXCR5$^+$ in areas of diffuse infiltration (Fig. 4*A*). In contrast, CCR7 was little expressed by few T cells and B cells, possibly because those cells lose their receptor on arrival to the GC. In addition, mature DCs (CD83$^+$) outside the lymphoid follicles were brightly stained (Fig. 4*A*).

Table III. *Chemokine receptor expression in T cell subsets from ITL, PBMCs from patients (AITDs) and from HD defined by RO and RA expression*

	Gate CD3$^+$		
	ITLs	AITDs, PBMCs	HDs,[b] PBMCs
CXCR4$^+$	59.6 ± 15.0	21.9 ± 15.1	58.3 ± 9.6
CXCR4$^+$RO$^+$	32.6 ± 10.7	5.1 ± 8.6	28.4 ± 10.6
CXCR4$^+$RA$^+$	10.4 ± 9.1	19.0 ± 18.4	30.6 ± 9.5
CXCR5$^+$	10.5 ± 8.7	10.2 ± 3.4	8.5 ± 4.2
CXCR5$^+$RO$^+$	7.1 ± 3.4	6.2 ± 4.1	6.1 ± 3.3
CXCR5$^+$RA$^+$	2.1 ± 1.9	6.9 ± 3.5	3.6 ± 1.8
CCR7$^+$	2.5 ± 1.4	39.3 ± 13.6	67.3 ± 7.9
CCR7$^+$RO$^+$	2.3 ± 1.6	8.9 ± 5.0	31.7 ± 13.0
CCR7$^+$RA$^+$	0.8 ± 0.7	32.6 ± 14.5	41.2 ± 12.6

[a] Values are given as mean ± SD of eight patients. Due to the effect of trypsin, which strips out a proportion of CD45RO and CD45RA molecules (see *Materials and Methods*), the percentage of CXCR4$^+$ in ITLs is higher than the sum of the RO and RA subsets. HDs, healthy donors; RO, CD45RO; RA, CD45RA.

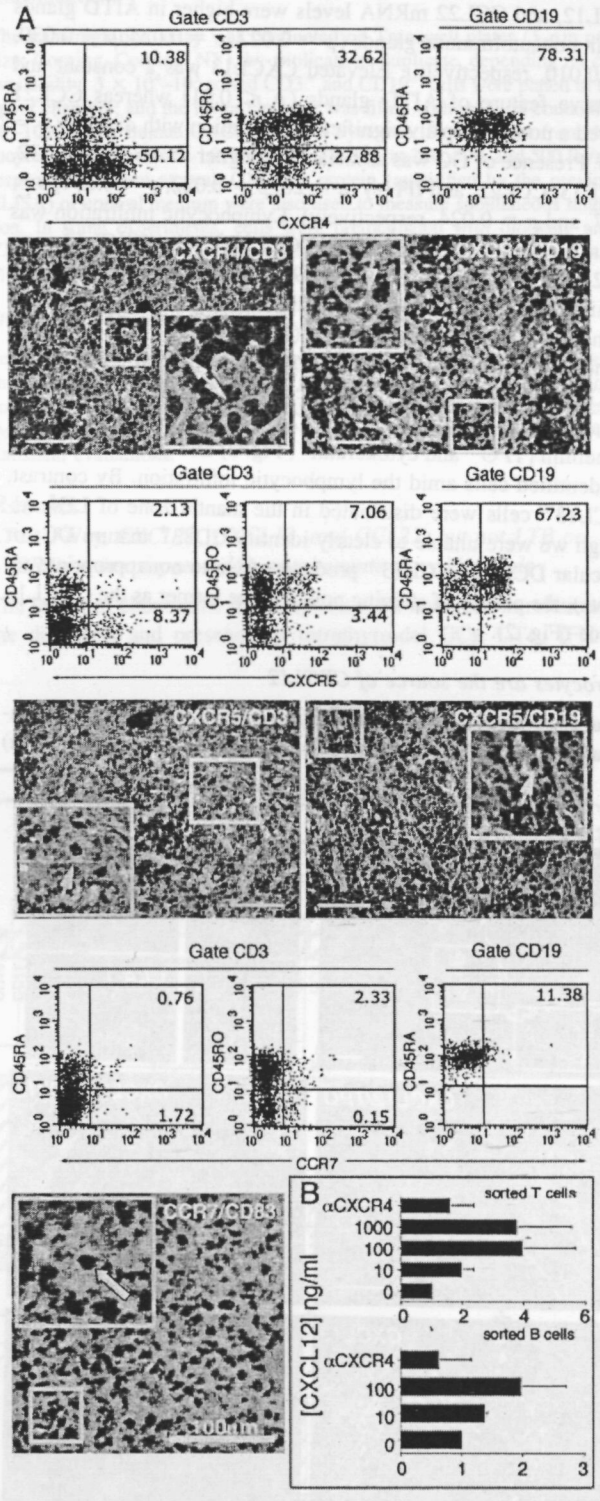

FIGURE 4. Expression of chemokine receptors in CD3$^+$, CD19$^+$, and CD83$^+$ thyroid-infiltrating cells. *A*, Dot plots of CXCR4, CXCR5, and CCR7 chemokine receptors and representative sections of their corresponding distribution by immunofluorescence in the intrathyroidal lymphoid follicles. Chemokine receptors are shown in red and CD markers are shown in green. A higher magnification is given in the insets of each panel; arrows indicate double-positive cells. *B*, CXCR4-mediated chemotaxis of sorted intrathyroidal T and B cells in a dose-dependent response to the CXCL12 chemokine (1–1000 ng/ml) and anti-CXCR4 blocking (100 ng/ml). The migration results are expressed as an index and are calculated as the ratio between the numbers of migrating cells in the sample referred to the spontaneous migration (mean ± SD from four independent experiments).

The CXCL12 receptor on ITLs is functional

Given that several factors (extracellular matrix, cell activation, soluble cytokines, and others) can determine molecular functions, we assessed the functionality of CXCR4 molecules on the surface of intrathyroidal B and T lymphocytes by chemotaxis assays with sorted $CD3^+$ and $CD19^+$ ITLs. Both sorted intrathyroidal T and B lymphocytes dose dependently migrated in a CXCL12α gradient, thereby confirming the functionality of CXCR4; maximal migration index was obtained at 100 ng/ml (33) for T cells and at 1000 ng/ml for B cells (Fig. 4*B*).

Marked peripheral reduction in $CCR7^+$ and $CD3^+CXCR4^+$ lymphocytes of AITD-GC^+ patients

The comparison between ITLs and PBMCs showed that $CXCR4^+$ lymphocytes were more abundant in the former (63.6 ± 12.9% vs 31.6 ± 12.9%; Fig. 5). This was due to their low proportion among circulating T cells (59.6 ± 15.0% vs 21.9 ± 15.1%; $p < 0.0001$); no such differences were found for B cells. This reduction of circulating $CXCR4^+$ T cells was particularly marked in the CD45RO subset (32.6 ± 10.7% vs 5.1 ± 8.6% $p < 0.001$; Table III). No significant differences in the proportion of $CXCR5^+$ cells were found when the main lymphocyte subsets were compared. The distribution of $CCR7^+$ cells was the opposite to that of CXCR4; $CCR7^+$ lymphocytes were significantly less abundant among ITLs than among PBMCs from the same patient (4.7 ± 2.8% vs 32.9 ± 15.1%; $p < 0.0001$), and this trend was found in both T cells and B cells (2.5 ± 1.4% vs 39.3 ± 13.6%, $p = 0.018$; and 11.4 ± 7.1 vs 39.8 ± 17.0 $p = 0.028$, respectively; Fig. 5).

Reference values for $CXCR4^+$ cells in secondary lymphoid tissue and control PBMCs suggested that the cause of this asymmetrical distribution was a striking reduction of circulating $CXCR4^+$

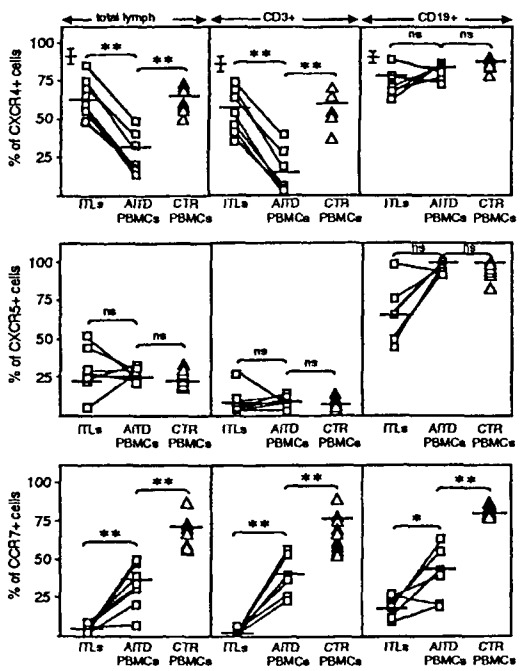

FIGURE 5. Chemokine receptor expression in ITLs and PBMCs from AITD patients and healthy donors (CTR). Data indicate the percentage of positive chemokine receptor expression. ITLs and PBMCs from the same AITD patient (□) are linked by a line; △, PBMCs from healthy donors; horizontal bars, mean of 8–10 independent experiments. *, $p < 0.05$; **, $p < 0.01$; ns, nonsignificant. As an additional reference, the mean ± SD of CXCR4-positive cells in lymph nodes from healthy donors is given with the symbol ⊣.

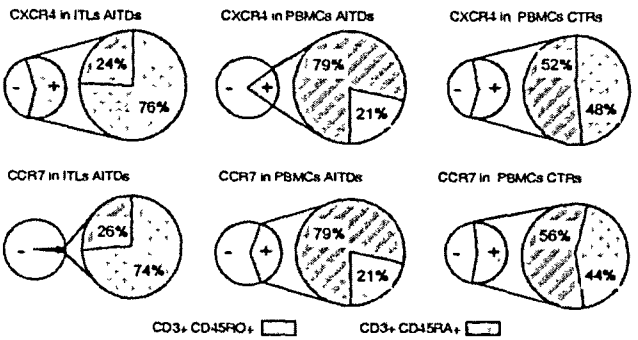

FIGURE 6. Relative representation of the distribution of $CD45RO^+$ and $CD45RA^+CD3^+$ cells in relation to CXCR4 and CCR7 expression in ITLs and PBMCs from autoimmune thyroid disease patients and from healthy donors. The small pie charts (*left*) show the relative proportion of chemokine receptor-positive (gray) and -negative (white) T cells. The large pie charts (*right*) show the percentage of $CD45RO^+$ and $CD45RA^+$ cells. Percentages are reported to the total number of $CD3^+$ cells.

T lymphocytes in AITD patients. To confirm this observation, we compared CXCR4, CXCR5, and CCR7 expression in PBMCs from this group of AITD patients ($n = 8$) with a group of sex- and age-matched healthy controls ($n = 8$). The results showed that the proportion of $CXCR4^+$ lymphocytes in AITD patients was about one-third of the controls (31.6 ± 12.9% vs 60.9 ± 7.8%; $p = 0.004$) due to a lower proportion of $CXCR4^+$ T cells (21.9 ± 15.1% vs 58.3 ± 9.6%; $p = 0.016$; Fig. 5), mainly affecting the CD45RO subset (5.1 ± 8.6% vs 28.4 ± 10.6%; $p < 0.0003$; Table III).

Regarding CXCR5, no significant differences were found between PBMCs from AITDs and healthy donors (23.1 ± 2.7% vs 19.1 ± 4.2%; $p = 0.391$; Fig. 5). The same applies to distribution analysis conducted among T and B cells and to the CD45RO and CD45RA T cell subsets.

The percentage of $CCR7^+$ cells was lower in AITD patients than in controls (35.3 ± 12.8% vs 68.5 ± 7.0%; $p = 0.0021$; Fig. 5). This was attributable to both the T cell (39.3 ± 13.6% vs 67.3 ± 7.9%; $p = 0.013$) and the B cell compartments (40.3 ± 17.0% vs 82.6 ± 3.8%; $p = 0.0005$; Fig. 5). Among T cells, the lowest proportion of $CCR7^+$ cells was found in the memory $CD45RO^+$ subset (8.9 ± 5.0% vs 31.7 ± 13.0%; $p = 0.006$; Table III).

To simplify the representation of results concerning the percentage of cells expressing CD45RA and CD45RO, the results were recalculated, and the graph was plotted taking the percentage of positive cells as 100% (Fig. 6).

Discussion

In rheumatoid arthritis, lymphoid neogenesis has been under intense scrutiny for clues that might explain the perpetuation of these diseases (11). We became interested in intrathyroidal lymphoid neogenesis as a part of TLT development, because it may help to explain how AITDs arise and are maintained despite a T cell repertoire tolerant to thyroid Ags (34). In a previous publication, we provided evidence suggesting that intrathyroidal LFs were functional and highly activated, and also that their B cells were specific for thyroid autoantigens (19). Our results clearly demonstrate that the main chemokines/cytokines involved in the generation of LFs are present at normal or above normal levels in intrathyroidal LFs, thus confirming the similitude to canonical LFs. Working with human tissues imposes several limitations, but we have tried to overcome them by studying a large number of samples from a

broad selection of patients and by testing in vitro the inferences derived from the observation of the pathological samples Overall, our results suggest that the development of ectopic lymphoid follicles in AITDs does not depend on a sole molecule but on the interplay of multiple factors Despite the parallelism between canonical and intrathyroid LFs, three differences merit discussion

1 The low number of $CCR7^+$-infiltrating lymphocytes which cannot be explained by the lack of high endothelial venules expressing CCL21, the initial event in LFs formation and prime chemoattractor of naive T cells (35), because we detected CCL21 in intrathyroidal high endothelial venules to an extent that is similar to those in other autoimmune (36, 37) or infectious diseases (38) The most plausible explanation is that once in the tissue, CCR7 is down-regulated, this would indicate indirectly that the lymphocyte turnover in intrathyroidal LFs is relatively low at this stage By contrast, CXCR4 and CXCR5 receptors remain expressed by both T and B cells, probably because of their role in maintaining the distribution of the different cell types in distinct areas of the intrathyroidal LFs

2 The lack of correlation of $LT\beta$ and $LT\beta R$ expression, factors known to play a fundamental role in the initiation of LFs, with the presence of ectopic LFs This difference, as the former, may be due to the late stage of maturation of the intrathyroidal LFs in our material In fact, by the time patients undergo surgery, the disease has been active for years, and therefore early events are not necessarily present

3 Thyrocytes are the main source of CXCL12 in AITD This is important but not totally unexpected because CXCL12 is an ancestral chemokine produced by a variety of cell types (24) Thyrocyte production of biologically active CXCL12 and infiltrating lymphocyte responsiveness to it are conclusively demonstrated by a combination of RT-PCR, immunofluorescent histochemistry, and chemotaxis techniques Thyrocytes can also produce CCL2 (macrophage chemoattractant protein-1) (39), CXCL19 (monokine induced by IFN-γ), and CXCL10 (IFN-γ-inducible protein-10) (40, 41), and this may explain why LFs arise so often in the thyroid gland even in MNG, a clinical entity of uncertain etiology It is conceivable that the initial event leading to the formation of intrathyroidal LFs is local nonspecific stress, e g , iodine overload as in nonobese diabetic mouse thyroiditis (42) Iodine may induce thyrocyte necrosis, which would stimulate resident macrophages to produce IL-1 and TNF, which may in turn induce CXCL12 synthesis by adjacent thyrocytes

The finding of a correlation between the levels of CCL21, CCL22, and CXCL13 and thyroid autoantibodies is well in agreement with our previous report of a correlation between the presence of intrathyroidal LFs and thyroid Ab titers (19) The capability of the thyroid tissue to express such a diversity of chemokines may contribute decisively to the local differentiation of autoreactive B cells and to the pathogenesis of AITDs This concept is also in line with the geographical view of immune response proposed by Zinkernagel et al (4), i e , the normal regional recirculation and distribution of lymphocytes would be crucial to prevent autoimmunity, and therefore its disruption, as here reported, may be a decisive event in the development of autoimmunity

The question of the formation of intrathyroidal LFs is part of a more general question of the reasons for the development of TLTs in many conditions Secondary lymphoid organs are designed to maximize the chances of a scarce Ag meeting a rare lymphocyte bearing the appropriate receptor When the immune system fails to create an efficient immune response against a highly localized Ag (e g , a microorganism), it may be advantageous to move a critical anatomical element of the immune response, the lymphoid follicle, to the site of the infection The stimulus that triggers lymphoid neogenesis may be the continuous production of cytokines and other inflammatory mediators by the stromal cells (43) TLTs lack the intricate circulation channels that distribute scarce incoming Ag through the lymph node They are probably not needed in TLT because their LFs are responding to local Ags that are both abundant and readily accessible (and this may be the main difference between TLTs and secondary lymphoid tissue) Lymphoid neogenesis in autoimmunity may be an undesirable consequence of this mechanism and may arise as results of chronic local stress (either mechanical stress in the joints or chemical stress in the thyroid) The formation of extranodal LFs does not inevitably lead to autoimmunity, because there is tolerance to local self-Ags, but breaking tolerance may be easier within these extranodal LFs because of the huge excess of Ag and the abundance of costimulatory signals (such as intrathyroidal chemokines) that may activate ever present low affinity T cells and B cells Unrestrained receptor revision occurring within these LFs may eventually lead to the formation of high affinity autoreactive B cells Intrathyroidal LFs are highly activated (19), and this is not surprising because there is plenty of Ag and inflammatory mediators to keep the reaction going

Finally, one of the most striking results from this work is the marked decrease in the proportion of circulating $CXCR4^+$ T cells and $CCR7^+$ lymphocytes, and the less marked but still significant reduction in $CXCR5^+$ B cells in AITD patients with ectopic LF These phenotypic changes may constitute good markers of the activity of the cellular immune response to the thyroid Ags and may be useful tests for the clinical assessment of the patients Ongoing work at our laboratory will determine whether this pattern of chemokine receptor expression in PBLs of AITD patients is a feature of the group whose glands contain LFs and also whether its is present in patients suffering other autoimmune diseases characterized by the formation of TLT

Autoimmune diseases are the end result of a multistep process in which genetic and environmental factors interact for a long time In humans, it is very difficult to define the main checkpoints, but organization of TLT may be an important step in the consolidation of an autoimmune response The data presented in this article define a broad and complex network of chemoattractant molecules determining the migration of lymphocytes to the thyroid and the formation of intrathyroidal lymphoid tissue, a process that, given its correlation with thyroid autoantibody levels and its repercussion in the phenotype of circulating lymphocytes, we believe constitutes a decisive checkpoint in the development of AITD

Acknowledgments

We thank the colleagues cited in the text for their generous donations of Abs and other reagents We thank Dr T Gallart for invaluable comments and conceptual discussion in several moments of our work, and also Dr C Martinez for the generous gift of reagents and protocol to perform CXCL12 ELISA We acknowledge the help of Dr A Lucas, Dr A Alastrue, and Dr J Escalante and their teams in collecting materials, Dr L Alcalde, Dr M Sospedra, Dr F Vargas, and L Muixí in tissue processing, and A Esteve for helping with statistics

References

1 Janeway C A , Jr , and R Medzhitov 2002 Innate immune recognition *Annu Rev Immunol 20 197*

2 Viret, C , K A Barlow, and C A Janeway, Jr 1999 On the intrathymic intercellular transfer of self determinants *Immunol Today 20 8*

3 Matzinger, P 2002 The danger model a renewed sense of self *Science 296 301*

4 Zinkernagel, R M , E S Aichele, S Oehen T Kundig and H Hengartner 1997 Antigen localisation regulates immune responses in a dose and time dependent fashion a geographical view of immune reactivity *Immunol Rev 156 199*

5 Pulendran B , R van Driel and G J Nossal 1997 Immunological tolerance in germinal centres *Immunol Today 18 27*

6 Han, S, B Zheng, J Dal Porto, and G Kelsoe 1995 In situ studies of the primary immune response to (4-hydroxy-3-nitrophenyl)acetyl IV Affinity-dependent, antigen-driven B cell apoptosis in germinal centers as a mechanism for maintaining self-tolerance *J Exp Med. 182 1635*

7 Hjelmstrom, P 2001 Lymphoid neogenesis de novo formation of lymphoid tissue in chronic inflammation through expression of homing chemokines *J Leukocyte Biol 69 331*

8 Murakami, J, Y Shimizu, Y Kashii, T Kato, M Minemura, K Okada, S Nambu, T Takahara, K Higuchi, Y Maeda, T Kumada, and A Watanabe 1999 Functional B cell response in intrahepatic lymphoid follicles in chronic hepatitis C *Hepatology 30 143*

9 Zaitoun, A M 1995 The prevalence of lymphoid follicles in *Helicobacter pylori* associated gastritis in patients with ulcers and non-ulcer dyspepsia *J Clin Pathol 48 325*

10 Crawford, D H, and S M McLachlan 1983 The relationship between the Epstein-Barr virus and rheumatoid arthritis *Br J Rheumatol 22 129*

11 Schroder, A E, A Greiner, C Seyfert, and C Berek 1996 Differentiation of B cells in the nonlymphoid tissue of the synovial membrane of patients with rheumatoid arthritis *Proc Natl Acad Sci USA 93 221*

12 Itoh, K, E Meffre, E Albesiano, A Farber, D Dines, P Stein, S E Asnis, R A Furie, R I Jain, and N Chiorazzi 2000 Immunoglobulin heavy chain variable region gene replacement as a mechanism for receptor revision in rheumatoid arthritis synovial tissue B lymphocytes *J Exp Med 192 1151*

13 Shione, H, Y Fujii, M Okumura, Y Yakeuchi, M Inoue, and H Matsuda 1997 Failure to down regulate Bcl-2 protein in thymic germinal center B cells in myasthenia gravis *Eur J Immunol 27 805*

14 Sims, G P, H Shiono, N Willcox, and D I Stott 2001 Somatic hypermutation and selection of B cells in thymic germinal centers responding to acetylcholine receptor in myasthenia gravis *J Immunol 167 1935*

15 Stott, D, F Hiepe, M Hummel, G Steinhauser, and C Berek 1998 Antigen-driven clonal proliferation of B cell within the target tissue of an autoimmune disease *J Clin Invest 102 938*

16 Wallace, W E H, S E M Howie, and A S Krajewaki 1996 The immunological architecture of B-lymphocytes aggregates in cryptogenic fibrosing alveolitis *J Pathol 178 323*

17 Ruddle, N H 1999 Lymphoid neo-organogenesis lymphotoxin's role in inflammation and development *Immunol Res 19 119*

18 Weetman, A P, and A M McGregor 1994 Autoimmune thyroid disease further developments in our understanding *Endocr Rev 15 788*

19 Armengol, M P, M Juan, A Lucas-Martín, M T Fernández-Figueras, D Jaraquemada, T Gallart, and R Pujol-Borrell 2001 Ectopic lymphoid follicles in thyroid autoimmune glands are sites of active B cell expansion and maturation relevance to pathogenesis *Am J Pathol 159 861*

20 McLachlan, S M, G Proud, C A Pegg, F Clark, and B Rees Smith 1985 Functional analysis of T and B cells from blood and thyroid tissue in Hashimoto's disease *Clin Exp Immunol 59 585*

21 Campbell, J J, and E C Butcher 2000 Chemokines in tissue-specific and microenvironment-specific lymphocyte homing *Curr Opin Immunol 12 336*

22 Tanabe, S, Z Lu, Y Luo, E J Quackenbush, M A Berman, L A Collins-Racie, S Mi, C Reilly, D Lo, K A Jacobs, and M E Dorf 1997 Identification of a new mouse β-chemokine, TCA4, with activity on T-lymphocytes and mesangial cells *J Immunol 159 5671*

23 Godiska, R, D Chantry, C J Raport, S Sozzani, P Allavena, D Leviten, and A Mantovani 1997 Human macrophage-derived chemokine (MDC), a novel chemoattractant for monocytes, monocyte-derived dendritic cells, and natural killer cells *J Exp Med 185 1595*

24 Bleul, C C, R C Fuhlbrigge, J M Casasnovas, A Aluti, and T A Springer 1996 A highly efficacious lymphocyte chemoattractant, stromal-cell derived-factor 1 (SDF-1) *J Exp Med 184 1001*

25 Gunn, M, V N N'go, K M Ansel, E H Ekland, G C Jason, and L T Williams 1998 A B cell homing chemokine made in lymphoid follicles activates Burkitt's lymphoma receptor-1 *Nature 391 799*

26 Ashhab, Y, O Domínguez, M Sospedra, C Roura Mir, A Lucas-Martín, and R Pujol-Borrell 1999 A one-tube polymerase chain reaction protocol demonstrates CC-chemokine overexpression in Graves' disease glands *J Clin Endocr Metab 84 2873*

27 Kokkotou, E, P Marafelia, E I Mantzos, and N A Tritos 2002 Serum monocyte chemoattractant protein-1 is increased in chronic autoimmune thyroiditis *Metabolism 51 1489*

28 Aust, G, D Sittig, M Steinert, P Lamesch, and T Lohmann T 2002 Graves' disease is associated with an altered CXCR3 and CCR5 expression in thyroid-derived compared to peripheral blood lymphocytes *Clin Exp Immunol 127 479*

29 Gouldvestre, C, F Batteux, and J Charreire 2002 Chemokines modulate experimental autoimmune thyroiditis through attraction of autoreactive or regulatory T cells *Eur J Immunol 32 3435*

30 Pujol-Borrell, R, I Todd, M Londei, A Foulis, M Feldmann, and G F Bottazzo 1986 Inappropriate major histocompatibility complex class II expression by thyroid follicular cells in thyroid autoimmune disease and by pancreatic β cells in type I diabetes *Mol Biol Med 3 159*

31 Belfiore, A, T Mauerhoff, R Pujol-Borrell, K Badenhoop, M Buscema, R Mirakian, and G F Bottazzo 1991 De novo HLA class II and enhanced HLA class I molecule expression in SV40 transfected human thyroid epithelial cells *J Autoimmun 4 397*

32 Monstein, H J, A G Nylander, and D Chen 1995 RNA extraction from gastrointestinal tract and pancreas by a modified Chomczynski and Sacchi method *BioTechniques 19 340*

33 Poznansky, M C, I T Olszak, R Foxall, R H Evans, A D Luster, and D T Scadden 2000 Active movement of T cells away from a chemokine *Nat Med 6 543*

34 Sospedra, M, X Ferrer-Francesch, O Domínguez, M Juan, M Foz-Sala, and R Pujol-Borrell 1998 Transcription of a broad range of self-antigens in human thymus suggests a role for central mechanisms in tolerance toward peripheral antigens *J Immunol 161 5918*

35 Gunn, M D, K Tangemann, C Tam, J G Cyster, S D Rosen, and L T Williams 1998 A chemokine expressed in lymphoid high endothelial venules promotes the adhesion and chemotaxis of naive lymphocytes *Proc Natl Acad Sci USA 95 258*

36 Christopherson, K W, 2nd, A F Hood, J B Travers, H Ramsey, and R A Hromas 2003 Endothelial induction of the T-cell chemokine CCL21 in T-cell autoimmune diseases *Blood 101 801*

37 Grant, A J, S Goddard, J Ahmed-Choudhury, G Reynolds, D G Jackson, M Briskin, L Wu, S G Hubscher, and D H Adams 2002 Hepatic expression of secondary lymphoid chemokine (CCL21) promotes the development of portal-associated lymphoid tissue in chronic inflammatory liver disease *Am J Pathol 160 1445*

38 Xanthou, G, M Polihronis, A G Tzioufas, S Paikos, P Sideras, and H M Moutsopoulos 2001 "Lymphoid" chemokine messenger RNA expression by epithelial cells in the chronic inflammatory lesion of the salivary glands of Sjogren's syndrome patients possible participation in lymphoid structure formation *Arthritis Rheum 44 208*

39 Kasai, K, N Banba, S Motohashi, Y Hattori, K Manaka, and S I Shimoda 1996 Expression of monocyte chemoattractant protein-1 mRNA and protein in cultured human thyrocytes *FEBS Lett 394 137*

40 García-López, M A, D Sancho, F Sánchez-Madrid, and M Marazuela 2001 Thyrocytes from autoimmune thyroid disorders produce the chemokines IP-10 and Mig and attract CXCR3$^+$ lymphocytes *J Clin Endocr Metab 88 508*

41 Romagnani, P, M Rotondi, E Lazzeri, L Lasagni, M Francalanci, A Buonamano, S Milani, P Vitti, L Chiovato, M Tonacchera, A Bellastella, and M Serio 2002 Expression of IP-10/CXCL10 and MIG/CXCL9 in the thyroid and increased levels of IP-10/CXCL10 in the serum of patients with recent-onset Graves' disease *Am J Pathol 161 195*

42 Hutchings, P R, S Verma, J M Phillips, S Z Harach, S Howlett, and A Cooke 1999 Both CD4$^+$ T cells and CD8$^+$ T cells are required for iodine accelerated thyroiditis in NOD mice *Cell Immunol 192 113*

43 Bottazzo, G F, R Pujol-Borrell, T Hanafusa, and M Feldmann 1983 Role of aberrant HLA-DR expression and antigen presentation in induction of endocrine autoimmunity *Lancet 2 1115*